BICEPS FEMORIS LONG HEAD ARCHITECTURE AND PASSIVE TISSUE STIFFNESS AND THEIR RELATIONS TO PERFORMANCE VARIABLES

Iida Laatikainen-Raussi

Master's Thesis in Biomechanics
Faculty of Sport and Health Sciences
University of Jyväskylä
Spring 2024

ABSTRACT

Laatikainen-Raussi, I. 2024. Biceps Femoris long head Architecture and Passive Tissue Stiffness and Their Relations to Performance Variables. Faculty of Sport and Health Sciences, University of Jyväskylä, Master's Thesis in Biomechanics. 68 pp.

The purpose of this master's thesis was to investigate the reliability of ultrasound elastography (SWE) imaging in passive muscles, changes in the shear modulus ("stiffness") along the *biceps femoris* long head (BFlh) muscle length, the architecture of the BFlh (muscle thickness (MT), fascicle length (FL) and pennation angle (PA)) and the relations of these muscle characteristics with performance variables (30 m speed, counter movement jump (CMJ), static jump, Nordic hamstring exercise, isokinetic hamstring:quadriceps-ratio). Hamstring injuries are common and cause a lot of absences, especially in sports involving high-intensity running. The hamstring muscles play a significant role in human movement, as they extend hip, flex knee, and participate in rotating the knee joint. BFlh, which is located laterally on the posterior thigh, is the most often injured hamstring muscle.

Ultrasound elastography (SWE) is a relatively new technology to evaluate tissue stiffness. The technique is based on the detection of shear waves; the propagation is faster the stiffer the medium. The validity and reliability of SWE in muscle and tendon imaging has been studied, but reporting varies. Mainly, it has been found to be a valid and reliable method, but it has its own limitations. All ultrasound measurements in this study were performed in one measurement session at rest. Participants of the study were female football (soccer) players (N=29).

The reliabilities of the ultrasound measurements (SWE and architectural measurements) were good to excellent (ICC for SWE 0.854, p=0.000; PA 0.935, p=0.000; FL 0.963, p=0.000 and MT 0.982, p=0.000). There were statistically significant differences in shear modulus along the BFlh in the right but not in the left leg. No high correlations were found between muscle architecture, shear modulus and performance variables. Some statistically significant moderate and low correlations were found, as relevant ones shear modulus and 30 meters sprint time (0.450, $p < 0.05$), fascicle length and jump performance (CMJ 0.379, static jump 0.441, $p < 0.05$).

The SWE measurements within the measurement session proved to be reliable, but the SWE measurement technology and analysis methods contain their own weaknesses. In the future, SWE may be a useful tool when monitoring muscle injury prevention and rehabilitation programs. Reliable comparisons between ultrasound measurements and performance variables require more precisely scheduled measurements and additional measurement methods (such as EMG) to support the findings. Imaging shear modulus closer to the muscle-tendon junctions could show greater intra-muscular differences in SWE measurements.

Keywords: shear wave elastography, reliability, hamstrings, muscle architecture

TIIVISTELMÄ

Laatikainen-Raussi, I. 2024. *Biceps femoriksen* pitkän pään arkkitehtuuri ja passiivinen kudosjäykkyys ja näiden yhteydet suorituskykymuuttujiin. Liikuntatieteellinen tiedekunta, Jyväskylän yliopisto, Biomekaniikan pro-gradu tutkielma, 68 s.

Tämän pro-gradu tutkielman tarkoituksena oli selvittää ultraäänielastografian (SWE) reliabiliteettia passiivista lihasta kuvattaessa, *biceps femoriksen* pitkän pään (BFlh) *shear modulusta* ("jäykkyyttä") pitkin lihaspituutta, BFlh:n arkkitehtuuria (lihaspaksuus (MT), fasikkelipituus (FL) ja pennaatiokulma (PA)) ja näiden lihasominaisuuksien yhteyksiä suorituskykymuuttujiin (30 m nopeus, kevennyshyppy, kyykkyhyppy, Nordic hamstring -liike, isokineettinen takareisi:etureisi -suhde). Takareisivammat ovat hyvin yleisiä ja aiheuttavat paljon poissaoloja erityisesti kovatehoisia juoksusuorituksia sisältävissä lajeissa. Takareiden lihakset ovat merkittävässä roolissa ihmisen jokapäiväisessä liikkumisessa, sillä ne ojentavat lonkkaa, koukistavat polvea ja osallistuvat myös polviniveltä kiertäviin liikkeisiin. Yleisimmin loukkaantuva lihas on nimenomaan BFlh, joka sijaitsee lateraalisesti reiden takaosassa.

Ultraäänielastografia (SWE) on hiljattain yleistynyt kuvantamisteknologia, jolla voidaan arvioida kudoksen jäykkyyttä. Menetelmä perustuu leikkausaaltojen havaitsemiseen, joiden eteneminen on nopeampaa mitä jäykemmässä väliaineessa ne etenevät. SWE:n validiteettia ja reliabiliteettia lihasten ja jänteiden kuvantamisessa on tutkittu, mutta raportointi on vaihtelevaa. Pääosin menetelmän on todettu olevan validi ja luotettava, mutta sillä on omat rajoitteensa. Kaikki tämän tutkimuksen ultraäänimittaukset suoritettiin yhdellä mittauskerralla levossa. Tutkittavat olivat naisjalkapalloilijoita (N=29).

Ultraäänimittausten (SWE ja arkkitehtuurimittaukset) reliabiliteetti oli hyvä–erinomainen (ICC SWE 0.854, p=0.000; PA 0.935, p=0.000; FL 0.963, p=0.000 ja MT 0.982, p=0.000). *Shear moduluksessa* pitkin BFlh:ta oli tilastollisesti merkitseviä eroja oikeassa, mutta ei vasemmassa jalassa. Muiden lihasominaisuuksien ja kudosjäykkyyden ja suorituskykymuuttujien välillä ei havaittu korkeita korrelaatioita. Joitakin tilastollisesti merkitseviä kohtalaisia ja matalia korrelaatioita havaittiin, olennaisimpina shear modulus ja 30 m sprinttiaika (0.450, $p < 0.05$), fasikkelipituus ja hyppysuorituskyky (CMJ 0.379, kyykkyhyppy 0.441, $p < 0.05$).

SWE-mittaukset mittauskerran sisällä osoittautuivat luotettaviksi, mutta menetelmän mittaus- ja analysointimenetelmät sisältävät omat heikkoutensa. SWE voi olla tulevaisuudessa käyttökelpoinen apuväline lihasvammojen ehkäisyn ja kuntoutuksen monitoroinnissa. Luotettavat vertailut ultraäänimittausten ja suorituskykymuuttujien välillä vaativat täsmällisemmin ajoitettuja mittauksia ja mahdollisesti muita mittausmenetelmiä (kuten EMG) tuekseen. SWE-kuvantaminen lähempää lihasjänneliitoksia voisi tuoda suurempia eroja *shear modulukseen* BFlh:n sisällä, ja kertoa näin lihaksen sisäisistä ominaisuuksista enemmän.

Avainsanat: elastografia, reliabiliteetti, takareidet, lihasarkkitehtuuri

ABBREVIATIONS

BFlh	biceps femoris long head
BFsh	biceps femoris short head
CMJ	counter movement jump
FL	fascicle length
H:Q	hamstring-to-quadriceps (ratio)
MTJ	muscle-tendon junction
NHE	Nordic hamstring exercise
PA	pennation angle
SM	semimembranosus
ST	semitendinosus
SWE	shear wave elastography
SWS	shear wave speed

TABLE OF CONTENT

1 INTRODUCTION

The hamstring complex includes *biceps femoris* (BF), *semimembranosus* (SM) and *semitendinosus* (ST) with BF consisting of short (BFsh) and long head (BFlh). Hamstring muscles play a very significant role in human movement, as they are particularly involved in hip extension and knee flexion (Rodgers & Raja 2019). In running, the hamstring muscles are activated especially at the end of the swing phase, when the hip is extended, and the knee extension is resisted (Koulouris & Connell 2005; Rodgers & Raja 2019). The power output is distributed between different muscles during running very individually (Avrillon et al. 2018; Hegyi et al. 2019).

Hamstring injuries are very common, especially in sports that include high-intensity sprints. The most frequently injured muscle is precisely the BFlh, and the majority of injuries are related to muscle-tendon junction. (Erickson & Sherry 2017.) For example, in football, hamstring injuries cause the greatest injury burden (absence days/1000 h) (Ekstrand et al. 2013). Therefore, examining the hamstrings and striving for effective injury prevention is important.

Ultrasound elastography is a relatively new imaging method. It is considered very potential for many applications, but more standardized protocols, analysis and interpretation are needed. Currently, the technique is used, for example to image liver fibrosis and breast injuries, such as tumors (Sigrist et al. 2017). It's been suggested to be an un-invasive tool for quantifying muscle properties (Lee et al. 2016). SWE (shear wave elastography) is based on measuring the velocity of shear waves in tissue (Sigristin et al. 2017; Taljanovic et al. 2017). Based on the speed of the waves, the shear modulus value can be calculated, and it describes the stiffness of the tissue (Taljanovic et al. 2017). Ultrasound elastography has been found to be a valid and reliable method for examining skeletal muscles (Chino et al. 2012; Eby et al. 2013; Mendes et al. 2018; Nakamura et al. 2016), but the reporting and methods of the studies vary significantly. Up to date, there are not many studies about performance and stiffness measured by SWE. Muscle architecture in the BFlh has been studied using ultrasound but there are some inconsistencies in the results regarding to differences along the muscle.

The purpose of this master's thesis was to study the reliability of ultrasound elastography within a measurement session when imaging passive muscle (BFlh). In addition, an effort was made to find out if there are relationships between the shear wave speed (stiffness), other architectural variables of BFlh and performance variables.

2 MUSCULUS BICEPS FEMORIS

Hamstring muscle complex has a significant role in human movement. The muscles of the complex are involved especially in hip extension and knee flexion. In gait pattern the hamstring muscles contract during the last quarter of the swing phase – they extend the hip and resist the knee extension. (Koulouris & Connell 2005; Rodgers & Raja 2019). With the anterior cruciate ligament (ACL), these muscles also stabilize the knee by resisting tibia moving forward during heel strike on the ground (Rodgers & Raja 2019).

2.1 Anatomy as a part of the hamstring complex

Biceps femoris (BF), *semimembranosus* (SM) and *semitendinosus* (ST) form the hamstring complex (figure 1). BF consists of two parts: short (BFsh, *caput brevis*) and long head (BFlh, *caput longum*). The hamstring muscles cross both; the hip and knee joints except the BFsh. It has been suggested that the BFsh woudn't be part of the hamstring muscles. (Rodgers & Raja 2019.) And, it has been noticed that some individuals don't have BFsh (Koulouris & Connell 2005). BFlh, SM and ST all attach in ischial tuberosity, and BFlh and ST have a common aponourosis with which they attach to their origo (Rodgers & Raja 2019). According to Woodley and Mercer (2005) it can be clearly noticed that BFlh attaches independently to the lateral fourth of the medial ischial tuberosity. The proximal tendons and origins are presented in figure 2.

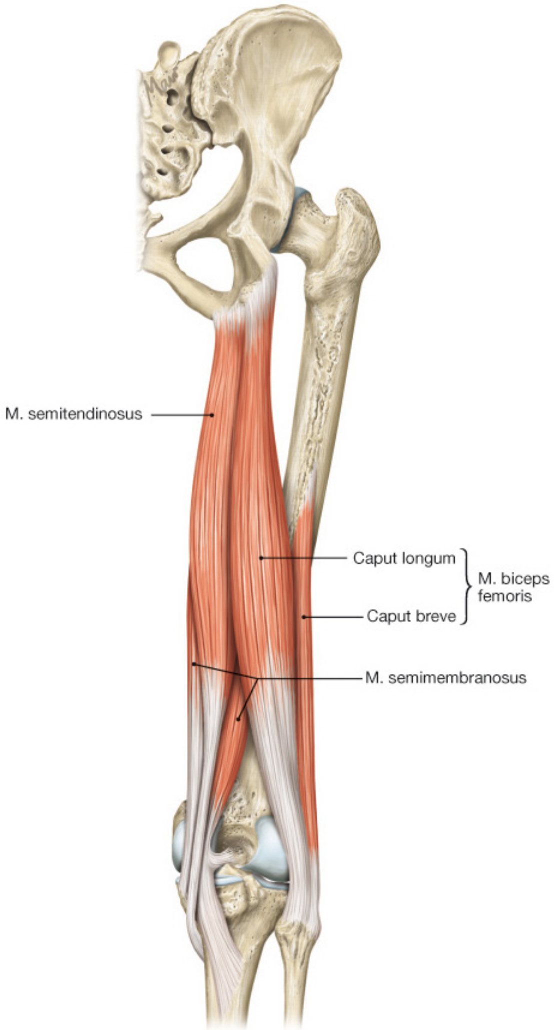

FIGURE 1. Hamstring muscles (Putz et al. 2010).

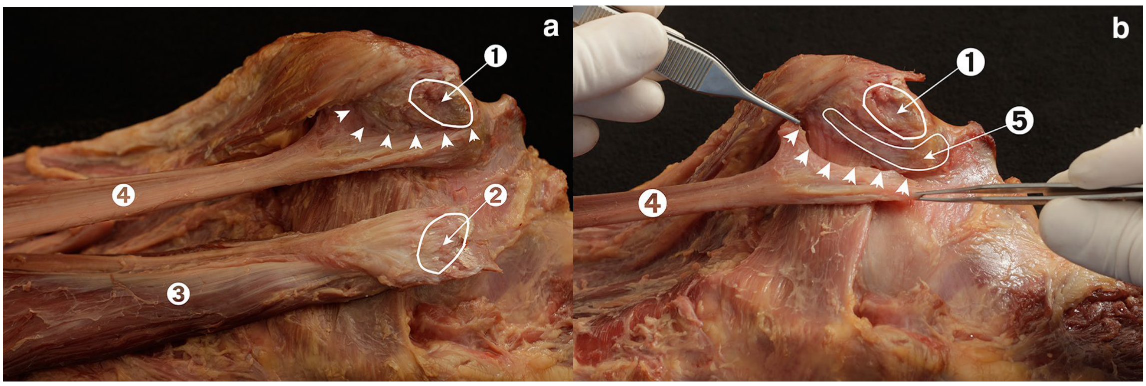

FIGURE 2. Proximal insertions and parts of hamstring muscle complex: 1) Origo for ST and BFlh 2) ST and BFlh tendon (attached to each other) 3) muscle-tendon junction 4) SM tendon 5) origo for SM (Stepien et al. 2018).

Insertions of BFlh are the head os fibula and the lateral condyle of tibia, insertion of ST is the medial tibia. *Pes anserinus* is the conjoined tendon for ST, *m. sartorius* and *m. gracilis* (see figure 3b) (Koulouris & Connell 2005). The distal tendon of semimembranosus has been reported to consist of three to eight branches. Straight branch, anterior branch, and the *ligamentum popliteum obliquum* are the most commonly mentioned. These insert to the posterior site of *tibial condyle*, to medial tibial condyle and to *ligamentum popliteum obliquum.* (Timmins et al. 2020.) In less than 50 % of people, part of the tendon of SM attaches to the posterior horn of lateral meniscus (Koulouris & Connell 2005). The distal tendons and the structures surrounding the knee joint are present in the figures 3a and 3b.

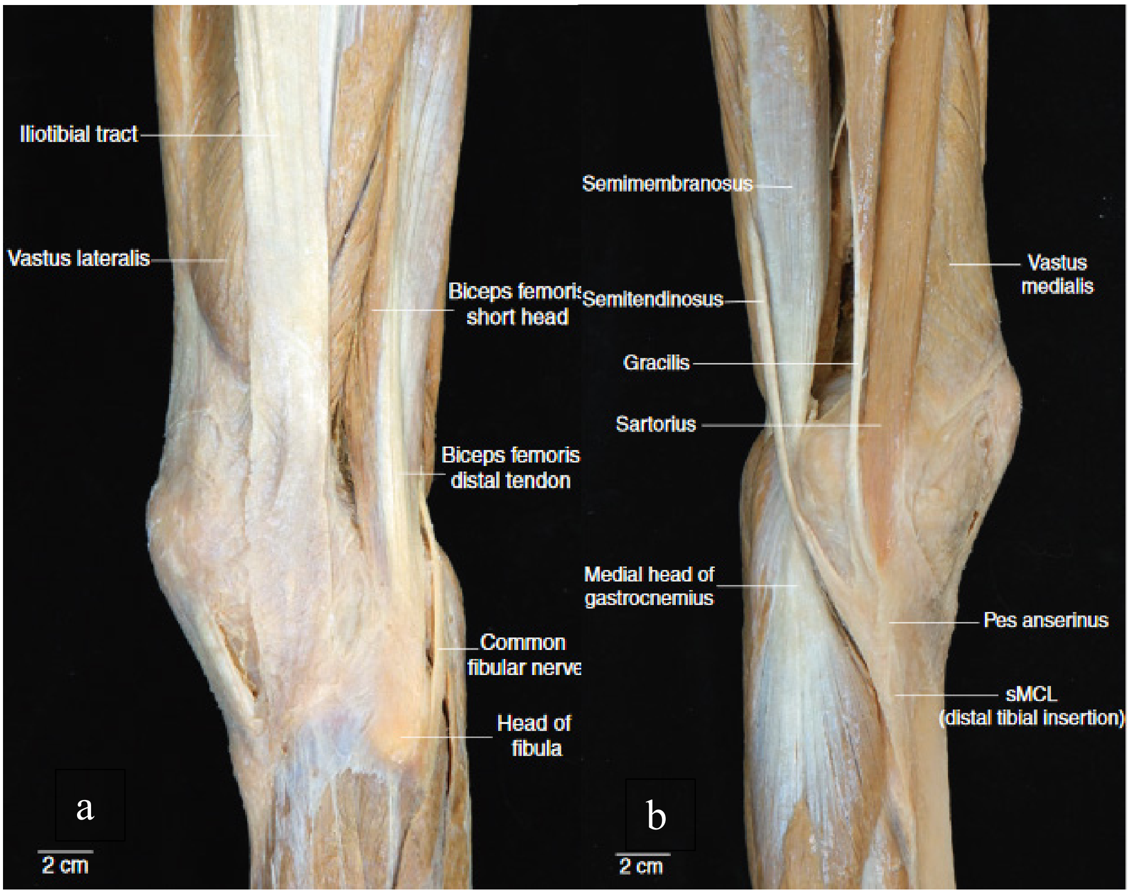

FIGURE 3a. The distal insertion of BF and FIGURE 3b. The distal insertions of SM and ST. (Timmins et al. 2020.)

The perforating branches of the deep femoral artery (*arteria profunda femoris*) are responsible for the vascular occlusion of the hamstring muscles. The branches of the iliac nerve (L3-S4) are responsible for the innervation. The tibial nerve innervates SM, ST and BFlh and the common peroneal nerve innervates the BFsh. (Rodgers & Raja 2019.) The origos, insertions, nerves, blood supply and functions of the hamstring muscles can be found from table 1.

TABLE 1. Anatomy of the hamstring muscles (Putz ym. 2009, s. 61).

	M. Biceps Femoris caput longum	M. Semitendinosus	M. Semimembranosus
Origo	Tuber ischiadicum	Tuber ischiadicum (lower medial surface)	Tuber ischiadicum
Insertion	Caput fibulae	Tuberositas tibiae (medial surface)	Medial tibia, several points
Function	Knee fexion, **lateral rotation**, hip extension and adduction (lateral rotation)	Knee flexion, medial rotation, hip extension (and adduction, medial rotation)	Knee flexion, medial rotation, hip extension (and adduction, medial rotation)
Nerve supply	N. ischiadicus, tibial part (plexus sacralis)	N. ischiadicus, tibial part (plexus sacralis)	N. ischiadicus, tibial part (plexus sacralis)

It has been noticed that ST and BF are not longitudinally homogeneous which may affect many properties measured. Assumptions of homogenous structure of these muscles may lead to incorrect interpretations of their function (Kellis et al. 2010.) From the distal parts SM consists mostly of muscle tissue with many half-pennate and multipennate muscle fibers and so, SM has many muscle fibers per unit area. The structure of ST, on the other hand, is quite thin, belt-like and very tendinous. (Koulouris & Connell 2005.)

BFlh is a fusiform muscle, and its fascicles have been reported to be longer on the more proximal than distal regions of the muscle. The reported pennation angles have some variation between articles. (Timmins et al. 2020.) According to Kellis et al. (2010) pennation angle is significantly greater in proximal than in distal parts of the muscle. In an ultrasound study by Tosovic et al. (2016), the BFlh pennation angle was significantly smaller in the most proximal site but the very distal site (90 % muscle length) versus the second distal site (70 % muscle length) seemed to show the opposite. Intra-observer reliability (repeated scans) for fascicle length (Tosovic et al. 2016; Oliveira et al. 2016), pennation angle (Tosovic et al. 2016; Oliveira et al. 2016) and thickness (Oliveira et al. 2016) seem to be very good-excellent.

2.2 Biomechanics

Hamstring muscles play a very significant role in human movement, as they are particularly involved in hip extension and knee flexion. Unlike SM and ST, the insertion of the BFlh is in the fibula and it takes part in knee joints lateral rotation. (Putz et al. 2009, p. 61.)

2.2.1 Running

As mentioned earlier, hamstring muscles are active especially during the last fourth of the swing phase in the gait pattern. They extend the hip joint and resist knee extension. However, the distribution of force output between the different hamstring muscles is very different between individuals (Avrillon ym. 2018; Hegyi ym. 2019), but similar between same individuals' different legs regardless of the dominant leg (Avrillon ym. 2018). Also, the muscle activity seems to distribute (between muscles and inside the muscle) in the same way when comparing different running speeds (Hegyi ym. 2019). EMG-activity in BFlh and ST increases along the muscle when the running speed increases. Increase in muscle-tendon complex length with the running speed is very small. When comparing BFlh EMG-activity in the late swing phase of running and maximal isometric contraction, the averaged activity in running is highest in the distal parts and lowest in the proximal parts of the muscle. (Hegyi et al. 2019.) Also, according to Morin et al. (2015), during the acceleration of running performance, the EMG activity of the biceps femoris increases in the late swing phase and in the first half of the contact phase. The activity of the gluteus maximus and vastus lateralis muscles, on the other hand, remains constant or decreases (Morin et al. 2015).

The eccentric peak contraction speed of the hamstring muscles is significantly higher in the late swing phase than in the late stance phase. The maximal muscle-tendon lengths are also greatest in the late swing phase (Thelen et al. 2005; Yu et al. 2008), but the muscle-tendon length during the peak contraction speed is greater during the support phase (Yu et al. 2008). The greatest relative length is in the BF muscle, and at high running speeds it is achieved in the late swing phase. However, the speed does not significantly affect the maximum length. (Thelen et al. 2005.)

In athletes familiar with high-intensity running performances, a higher average GRF (ground reaction force) has been observed in those who are able to activate their hamstring muscles strongly just before ground contact, and who have the greatest capacity to produce eccentric force in the hamstrings. The EMG activity of the hamstrings during and at the end of the swing phase, as well as the peak torque of the eccentric knee flexion are therefore related to the magnitude of the horizontal GRF. This is due to the backward movement of the foot just before ground contact. (Morin et al. 2015.)

Morin et al. (2015) states that the hip extensors and especially the muscles of the buttocks should be carefully considered in the training of athletes, because they are of great importance for sprint acceleration, and their risk of injury is significant. Increasing the power output of eccentric knee flexion and concentric hip extension can be an effective way to improve running acceleration. Repeated high-intensity running performances are essential in many sports, so it would be interesting to study activity and power generation capacity also in connection with such fatigue. (Morin et al. 2015.) For example, in soccer, there are a lot of high-speed running performances during the game; in top-level soccer players, 217 ± 13 runs at a speed of 18-30 km/h and 39 ± 2 sprints over 30 km/h during the game. For middle-class players, the numbers are slightly lower (171 ± 7 and 26 ± 1 pcs). (Mohr et al. 2003.)

The function and importance of the hamstrings in high-intensity running performances can be understood based on the above. The coordination of the hamstring muscles has also been found to affect endurance performance; the greater the imbalance between the ends of the muscles, the worse the muscle endurance (Avrillon et al. 2018).

2.2.2 Nordic hamstring exercise

Nordic hamstring exercise is an eccentric exercise where the knee joint is the only moving joint. Ankles are strapped or held, knees are extended slowly with straight hips and middle body. So, the hamstrings decelerate the movement and work against gravity. The movement requires strong isometric work from the core muscles to support the middle body (spine and hip joints). The movement is shown the figure 4. According to Hegyi et al. (2018) the distal regions of BFlh have the highest activity levels during NHE. For ST the activity levels between distal and proximal regions are the opposite.

NHE has been shown to be a useful exercise in the prevention of hamstring injuries. According to a systematic review from Al Attar et al. (2017), soccer teams using an injury prevention program including NHE have a decreased risk (51 %) of hamstring injuries compared with teams which do not use injury prevention program.

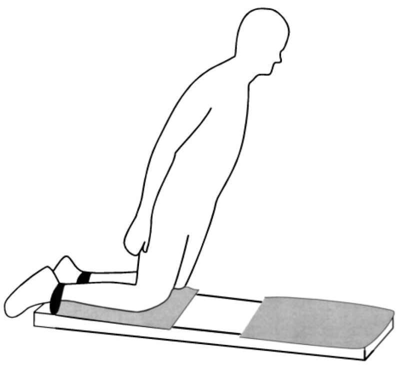

FIGURE 4. NHE. Figure by Brockett et al. (2001) who were the first introducing NHE (Ditroilo et al. 2013).

2.2.3 Isokinetic hamstring:quadriceps ratio

The isokinetic hamstring-to-quadriceps (H:Q) ratio is a measure used to assess the balance between the hamstrings and quadriceps muscles during knee movements. The ratio has been expressed as the strength of the concentric contraction of the hamstrings relative to the quadriceps (conventional) (for example Liporaci et al. 2019; Andrade et al. 2021), or as the strength of the eccentric contraction of the hamstrings relative to the concentric contraction of the quadriceps (functional) (for example De Ste Croix et al. 2018; Eustace et al. 2019). The movement is velocity dependent and different velocities have been used. Some thresholds for injury risk and prevention have been established. A study suggest that in elite football players H:Q conventional ratio with 60 °/s less than 55 % or over 64 % increases muscle injury risk by 7.49-46.94 (Liporaci et al. 2019). Typically, 60 % is suggested to be the minimum for the conventional ratio. Based on a review concerning professional male soccer players, H:Q functional ratio should be around 80% when tested at an angular velocity of 60 °/s. For tests conducted at intermediate to fast angular velocities (120 °/s-300 °/s), the expected values are between 100–130 %. (Baroni et al. 2020.)

2.3 Injuries

Hamstring injuries are common in athletes of all ages, in all kinds of sports and at all different levels of competition. The diagnosis of the injury is usually made based on the patient's history, physical examination, and imaging. There are proven methods to prevent injuries. (Ahmad et al. 2013.) The increased physical activity of the general population and the high demands of athletes have increased the prevalence of hamstring injuries, and a wide variety of injuries are observed. The development of imaging methods and the increase in usability have also increased research on the hamstring muscles. Magnetic resonance imaging and ultrasound are considered the best imaging methods. (Koulouris & Connell 2005.)

For example, in Australian football more than 90 % of hamstring injuries are sudden (Verrall et al. 2003). The risk of acute hamstring strain injuries is high in sports that involve sprinting, kicking, or high-speed skill-demanding movements such as American football, soccer, rugby, and track and field. The risk of injury has also increased in sports that involve extensive stretching, such as dance. (Erickson & Sherry 2017.) In a study conducted in dance, all hamstring injuries occurred during slow hip extensions with a straight knee (Askling et al. 2007b). In outdoor sports (e.g. football), the risk has been found to be higher than in indoor sports (e.g. basketball and volleyball) and most injuries occur in competitive situations. (Erickson & Sherry

2017.) Jumping and kicking can also influence the risk. According to a systematic literature review by Storey et al. (2012), in sprints BFlh is the most frequently injured muscle alone or simultaneously with ST. SM injuries, on the other hand, are common in sports involving slow stretches. In most cases, muscle-tendon connections are related to the injury site, and proximal structures are damaged more often than distal ones. (Storey et al. 2012.)

In football, for example, hamstring injuries are very common and often lead to absences from games or training. Based on data collected during the 2010 FIFA World Cup, hamstring strains were the most common cause of absences from both games and training injuries. Data was collected from all World Cup final teams (32 teams). (Dvorak et al. 2011.) In a long follow-up study of 11 years, hamstring muscle injuries were the most common among elite football players (12.8% of injuries), and the burden caused by them (absence days/1000 h) was clearly the greatest (Ekstrand et al. 2013). In elite athletes, the majority of hamstring injuries target the BFlh muscle; 84% BF, 11% SM and 5% ST (Ekstrand et al. 2012), respectively 83%, 10%, 7% (Koulouris et al. 2007) and BFlh 81% (Verrall et al. 2003). On the other hand, most of the muscle injuries of the hamstrings of the dancers targeted the SM (87%) and the quadratus femoris (87%). All SM's injuries were related to its proximal tendon. (Askling et al. 2007b.)

Anatomical differences within the BFlh are large. Especially at high running speeds, the proximal part of the muscle is subjected to greater stress than the rest of the muscle (Fiorentino et al. 2014), and most hamstring injuries are related to the proximal muscle-tendon junction (Askling et al. 2007a; Koulouris et al. 2007). For example, when studying the Nordic hamstring movement, Hegyi et al. (2018) found that the EMG activity of the proximal part of the BFlh was the smallest, which may be connected to a greater stretch near the proximal muscle-tendon junction in cyclic knee flexion-extension contractions. Hamstring strains during running are most likely to occur during the late swing or stance phase. There a high eccentric contraction speed is combined with a lengthened muscle-tendon complex. (Yu et al. 2008.) Koulouris and Connel (2005) also state, referring to Slocum and James (1968), that the quick change of the hamstrings from a stabilizing role to flexion and extension has been considered an essential cause of injuries. Since the muscles cross two joints, their contraction cannot be limited to just one joint either. Differences between the muscles in the lever arm to the hip and knee may explain the greater susceptibility of BF to injury. For all hamstring muscles, hip flexion lengthens the muscle during the swing phase. In the late swing phase, knee flexion shortens the muscles, but because the BF has a smaller knee flexion lever arm, it shortens less. (Thelen et al. 2005.)

Opar et al. (2012) have compiled risk factors for hamstring injuries in their review article. Being over 24-year-old increases the risk of injury significantly, at least in Australian football and football. Bilateral asymmetry has been found to be a risk factor in American football players, track and field athletes and football players (asymmetry over 8-15%). There is no clear consensus on the connection between force production and hamstring injury risk; based on animal experiments, a fully activated muscle withstands greater tension than a partially activated muscle, but on the other hand, in some human studies, a weaker maximal knee flexion force in relation to body weight has been found to be a risk factor. A low hamstring-quadriceps force ratio is a risk factor for hamstring strain injuries. When investigating the importance of mobility on injury risk, conflicting results have been obtained. Fatigue, on the other hand, has been found to be a significant risk factor, as more injuries occur in the final stages of competitive games or training. (Opar et al. 2012.) In athletes, a shorter fascicle length in the BFlh predisposes to hamstring strain injuries (Timmins et al. 2015). Also, BFlh fascicle length seems to be shorter in the previously injured limb than the contralateral one. According to Sarto et al. (2021) one limitation in the fascicle length studies is the linear extrapolation method used with normal ultrasound pictures with limited field of view, and more appropriate imaging techniques (EFOV3D US or diffusion tensor imaging for example) should be used in future studies.

3 SHEAR WAVE ELASTOGRAPHY

Tissue stiffness is a changed due to various diseases and conditions. Clinically, it is useful to measure tissue stiffness for example to early detect and differentiate diseases, improve the accuracy of diagnosing diseases including fibrosis and to assess responses to some treatments. (Shiina et al. 2015). The first commercial device for elastography was available in 2003 and the use and development of elastography techniques has developed rapidly in the past 20 years (Cui et al. 2022).

Ultrasound elastography techniques are divided into three categories by The World Federation for Ultrasound in Medicine and Biology (Ferraioli et al. 2018): strain elastography (SE), transient elastography (TE) and acoustic radiation force impulse (ARFI). In SE the tissue deformation is evaluated by manual compression or physiological motion and the strain is measured. In TE an external vibration generates a shear wave and in ARFI technique the shear waves are produced by acoustic radiation force. The speed of the shear waves is measured in both techniques. ARFI is divided further into point shear wave elastography (p-SWE), 2D shear wave elastography (2D SWE), and 3D shear wave elastography (3D SWE) techniques. (Cui et al. 2022.) In Shiina's et al. (2015) review the classification is a bit different and ARFI is divided into ARFI imaging (under strain imaging) and point shear wave speed imaging and shear wave speed imaging (two last ones being referred the quantitative ARFI methods). The classifications can be found in the table 2. Table 3 supplements the information in table 2. In this thesis the focus will be on the 2D SWE/shear wave speed imaging because it is the method used in the study. Shear wave elastography is regarded as being more objective, quantitative, and reproducible compared to compression sonoelastography, with its increasing applications to the musculoskeletal system (Taljanovic et al. 2017) and B-image guidance during acquisition with only one transducer in use (Cui et al. 2022).

In general, ultrasound elastography can be used to determine tissue elasticity, i.e. the ability to resist changing shape due to external force or the ability to return to its original shape after the force applying has stopped. Ultrasound elastography is roughly divided into two techniques, strain imaging and shear wave imaging. There are three different imaging techniques that utilize shear waves, of which 2D shear wave elastography, abbreviated SWE, is discussed here. (Sigrist et al. 2017.)

TABLE 2. Different elastography methods (modified from Shiina et al. 2015). *The term ”ARFI” is used to refer to the use of ARFI excitation and measuring either strain/displacement or shear wave speed. “ARFI imaging” refers to the use of ARFI excitation and measurement of tissue displacement. **In point SWS measurement a local average of SWS is determined using ARFI excitation. A specific ROI is used, and it is assumed homogenous. ***There is point SWS measurement in transient elastography too. The name refers to the excitation method (dynamic nature).

Measured physical quantity	Strain or displacement 		Shear wave speed 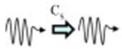	
Methods	**Strain Imaging**		**Shear wave imaging**	
Excitation methods				
Manual compression -palpation -cardiovascular pulsation -respiration	**Strain elastography**		N/A	
	ElaXtoTM	Esaote		
	Real-time tissue elastographyTM	Hitachi aloka		
	Elastography	GE, Philips, Toshiba, ultrasonix, Mindray		
	ElastoScanTM	Samsung		
	eSieTouchTM	Siemens		
	Elasticity Imaging 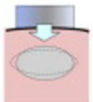			
Acoustic radiation force impulse excitation	*ARFI Imaging		**Point shear wave speed measurement (Average shear wave speed in a region of interest)	
	Virtual TouchTM Imaging (VTI/ARFI)	Siemens	VirtualTouchTMQuantification (VTQ/ARFI)	Siemens
	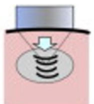		ElastPQTM	Philips
			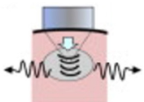	
			Shear wave speed imaging	
			ShearWaveTMElastography (SWETM)	SuperSonicImagine
			Virtual TouchTM Image Quantification (VTIQ/ARFI)	Siemens
Controlled external vibration			**Transient elastography (Point ahear wave speed measurement)**	
			FibraScanTM	Echosens
			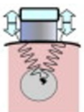	

TABLE 3. Elastography output (modified from Shiina et al. 2015).

Methods Excitation method	Strain imaging	Shear wave imaging
Manual compression - palpation - cardiovascular pulsation - respiratory	**Strain elastography** Strain or normalized strain Geometric measures Strain ratio E/B size ratio	
Acoustic radiation force impulse excitation	**ARFI Imaging**	**Point shear wave speed measurement**
	Displacement or normalized displacement Geometric measures Displacement ratio E/B size ratio	Shear wave speed (m/s) Young's modulus (kPa) **Shear wave speed imaging** Shear wave speed (m/s) Young's modulus (kPa)
Mechanical external vibration		**Transient Elastography** Young's modulus (kPa)

3.1 Principle

This chapter gives a cursory review of the principles of SWE. More detailed mathematical background of SWE technology is discussed for example in an article by Sarvazyan et al. (1998).

The elasticity of soft tissues is usually expressed by elastic moduli: Young's modulus (E) and shear modulus (G). Elasticity describes how the tissue resists the deformation created by compression or shear. To calculate the moduli, one of the following equations are typically used:

1) Hooke's law: $\sigma = \Gamma \cdot \varepsilon$ where σ is stress (external force per area), ε is train and Γ is the elastic modulus. And then calculating E using the following equation: $E = {}^{\sigma}/_{\varepsilon}$ where σ is externally applied stress and ε measured strain.
2) Calculating E or G using the following equation: $E = 2(1+v)g = 3G = 3\rho c_s^2$, where v is the Poisson's ratio which is 0.5 for an incompressible medium and is assumed the

same for soft tissue as an approximation, ρ is the tissue density and c_s is the propagation speed. (Shiina et al. 2015.)

In shear wave imaging the propagation of shear waves in the material (tissue) is monitored. Shear waves' propagation direction is orthogonal to the tissue displacement direction (unlike in the other methods). The speed of shear wave propagation is related to the stiffness of the tissue as in the second equation above. (Shiina et al. 2015.)

The basic physics of SWE is briefly explained in the figure 5. In step one the linear ultrasound array generates shear waves by acoustic radiation force. As said and seen in the figure, shear waves propagate perpendicularly (SW arrows). In the second step the displacement and velocity are tracked using fast plane excitation. Displacement of the tissue is calculated using a speckle tracking algorithm. (Taljanovic et al. 2017.)

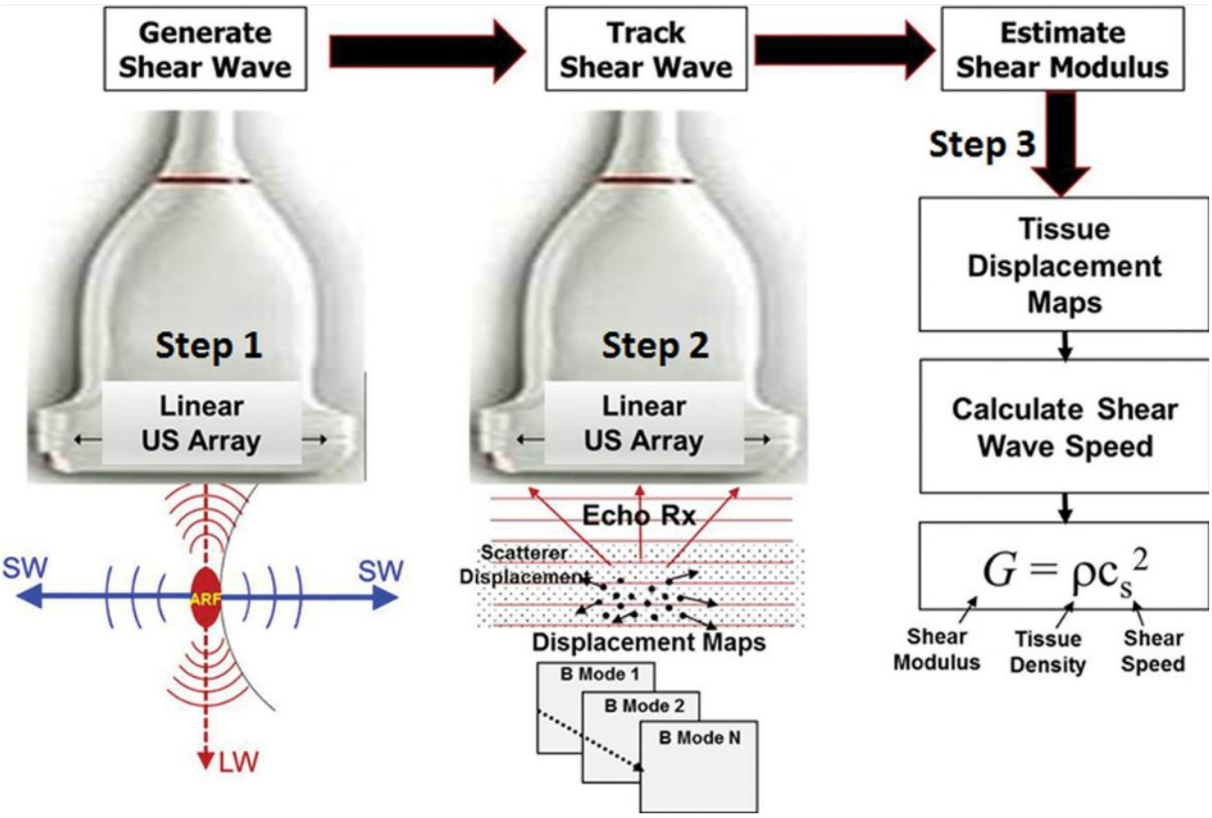

FIGURE 5. Basic principles of SWE (Taljanovic et al. 2017).

In step 3, maps of tissue displacement are used to determine shear-wave velocity (cs), often stated in meters per second. The shear-wave velocity distribution at each pixel correlates directly with the shear modulus (G). The shear modulus is computed using a straightforward mathematical equation and represents the stiffness and elasticity of the tissue, expressed in units of pressure, typically kilopascals.

Shear waves propagate in soft tissue much slower (~ 1000 times) and attenuate much faster (~ 10000 times) than ultrasound waves. Shear wave speed can be observed if the ultrasound echoes are generated with big enough frequency. (Taljanovic et al. 2017.) Differences between elastography techniques and different manufacturers devices makes comparing of the results (for example cutoff values) difficult (Sigrist et al. 2017; Cui et al. 2022). According to Sigrist et al. (2017) Shear Wave™ Elastography by SuperSonic Imagine (SSI) is the most valid device to estimate liver fibrosis.

Limitations of SWE imaging are the depth of imaging, in some devices defining the region of interest (ROI), sensitivity of outside pressure and the transducers orientation in relation to the structures being studied. If there is void in the elastography ROI, the frame rate may be too low or the void is present due to fluids, for example blood or edema (typical in superficial structures). (Taljanovic et al. 2017.) In addition, the commercial devices make many assumptions of the tissue. According to these, tissue is linear (stretch increases linearly as a function of stress), elastic (deformations do not depend on the rate of tension and the tissue returns to its original state, equilibrium), isotropic (symmetric and homogeneous and responds to tension in same way from all directions), and uncompressible (the total volume remains constant). In some clinical trials these assumptions work fine but in some cases all of them are violated. (Sigrist ym. 2017.)

SWE is potential and developing technique (Taljanovic et al. 2017; Sigrist et al. 2017; Cui et al. 2022). Methodology needs standardization for future research (Sigrist et al. 2017; Cui et al. 2022).

3.2 Validity and reliability with muscle tissue

In quantitative research, validity tells whether the meter or a device measure exactly the desired thing (Heale & Twycross 2015). Reliability tells how repeatable the measurement or device is

(Hopkins 2000, Heale & Twycross 2015); the better reliability, the more accurate are the single measurement and the changes are easier to detect (Hopkins 2000). Thereby, both validity and reliability have a significant role when evaluating the quality of studies.

At the end of 2010s using ultrasound elastography technique for skeletal muscle imaging has increased rapidly. Information is obtained real time, and measuring is possible from active and passive muscles. Thus, elastography is the most promising way to assess muscle properties. (Ryu & Jeong 2017.)

Ultrasound elastography has investigated to be valid method for measuring tissue hardness/stiffness (Chino et al. 2012; Eby et al. 2013; Nakamura et al. 2016) but the methods and reporting of the validity are very variable. Chino et al. (2012) measured stiffness of tissue mimicking materials with SWE and the Young's moduli values were confirmed by the manufacturer using the mechanical displacement–load compression method with two types of devices with good correlations in Young's modulus ($r = 0.996$, $p = 0.001$). Eby et al. (2013) measured the stiffness of swine's brachialis whole-muscle samples simultaneously with SWE and tensile test using a material testing system to stretch the tissue. Nakamura et al. (2016) measured SWE of medial gastrocnemius muscle and determined the MTJ (myotendinous junction) displacement using ultrasound B-imaging during passive dorsiflexion of ankle; the movement of MTJ and the shear modulus of MG are highly correlated with each other ($r = 0.964$, $p = 0.036$). All three studies used different devices for SWE.

Eby et al. (2013) have investigated SWE validity when measuring muscles. Stiffness measured by both SWE and the traditional material testing method (MTS) increased with increasing tensile load. The methods also correlate well with each other throughout the tensile load scale when the ultrasound probe is parallel to the muscle fascicles. The shear modulus changes significantly when the probe is at 45° angle to the fascicles, but even then, the measurements are repeatable. (Eby et al. 2013.) According to Miyamoto et al. (2015), the angle of the probe is not important for isotropic material, but it is small for muscle tissue (1.3% of the measured values). For measuring muscles, the method is considered valid as long as the deviation of the probe from the direction of the muscle fascicles is less than 20°. According to Ruby et al. (2019), the muscle tension and fascicle orientation, depth and ROI size influence the SWV (shear wave velocity) significantly, as well as the software choice.

To find out more about the reliability of the SWE, a systematic literature search was done for this thesis. The search was done during spring 2023 with ”(”*shear wave elastography*”) AND *muscle*” on titles and abstracts from three databases: PubMED, Web of Science and Scopus. All together there was 2057 results and after excluding doublets the number of articles were 957 from which 7 weren’t written in English. From the remaining articles, titles and abstracts were screened, and color coded to be read more precisely if the article included (or could likely include) shear wave elastography, human muscles, reliability/reproducibility. To include the article to the table below, the criteria were: measuring healthy human skeletal muscles (excluding articles concerning only diaphragm or pelvic floor/urethral sphincter muscles), studying reliability and reporting ICC, using shear wave elastography. Many articles were related to cerebral palsy, stroke patients or in some way spastic muscles. These articles were excluded. After evaluating the articles with the mentioned criteria, 34 articles were left for the table 4. In addition to the articles in the table, there are studies in which reliability is reported, but there is no mention of it in the abstract and it is only a small side note in the paper. All the articles were evaluated by only one reader (Laatikainen-Raussi) to make the choice of including.

TABLE 4. SWE reliability in human skeletal muscles, continuous until page 23 (Laatikainen-Raussi 2024).

Authors	Year	Muscles studied	ICC model	Results
Alfuraih et al.	2018	VL, BF, biceps brachii (BB), and abductor digiti minimi muscles	ICC(1,k)	VL: 0.77 (0.52, 0.90), BB: 0.91 (0.82, 0.96), BF 0.90 (0.79, 0.96), ADM 0.97 (0.94, 0.99)
Alfuraih et al.	2017	Rectus femoris (RF), different parts	ICC(1,1) and ICC3,3 (inter-device)	Intra-device: 0.92–0.98 (0.82–0.99) depending on the location, inter system: 0.43-0.71 (0.18-1)
Baumer et al.	2017	Supraspinatus, relaxed and active	inter-user, intra-user, and inter-day repeatability	ICC > 0.87, day-to-day > 0.33 for passive muscle, > 0.65 for active muscle
Bedewi et al.	2021	Anterior and middle scalene muscles	2-way random effect	Intra-rater: 0.80
Blain et al.	2019	Multifidus and erector spinae, 5 postures, right and left	Intra-session (repeated 3 measures)	ICC 0.386-0.862 (0.060–0.949), lower in multifidus
Bravo-Sánchez et al.	2021	VL, relaxed	Intra-day ICC(2,1) (1h), inter-day ICC(3,1) (1d)	Intra-day 0.80, 0.68-0.88, CV 15.3%, SEM 3.17 kPa, inter-day 0.62, 0.41–0.77, CV of 33.8%, SEM 5.60 kPa
Creze et al.	2019	Multifidus (S1 and L3), longissimus, different positions	Intra-rater, three repeated measures and inter-session	Wide range depending on position and muscle, ICC -0.06–0.95, inter-day 0.28-0.56
Dubois et al.	2015	Lateral gastrocnemius, VM, rested and stretched	ICC(2,1)	ICC inter 0.87–0.91, CV 8–11 %, Intra 0.91–0.94, CV 7–8 %
Dulgheriu et al.	2022	Soleus and deltoideus	ICC(2,k)	0.912 (0.891–0.929)
Hatta et al.	2015	Supraspinatus, cadaveric shoulders, 0° abduction and 0° rotation	Intra- (ICC1,1) and inter-observer (ICC2,1)	Intra 0.945–0.970, inter 0.882–0.948, CV among overall measurements 4.93 (3.05) %
Kelly et al.	2018	Infraspinatus, erector spinae, and gastrocnemius (rest and 40, 80 %MVIC)	ICC(3,1), ICC(3,3)	0.46–0.98 (95% CI 0.23 to 0.95)

Authors	Year	Muscles studied	ICC model	Results
Klauser et al.	2022	Tensor fasciae latae (TFL), medial gastrocnemius (MG) (and ITB)	two-way mixed effects, absolute agreement of measurements	Intra-rater: TFL: 0.98 (0.96–0.99), GM: 0.87 (0.80–0.92)
Koo et al.	2014	Tibialis anterior (TA)	ICC(3,1)	Elasticity–angle relationship, ICC in slack angle 0.852, CV of SWE 1.92 %
Koppenhaver et al.	2018	Erector spinae at rest, lumbar multifidus at rest, minimal, moderate, and maximal contractions	Intra-rater ICC(3,1), (3,3) (repeated 3 measures), test-retest ICC(2,1)	ICC(3,1) 0.53-0.79 (0.33–0.88), ICC(3,3) 0.77–0.92 (0.60–0.96), ICC(2,1) 0.51–0.66 (0.13–0.81)
Kozinc & Šarabon	2020	Trapezius, relaxed, shoulder abducted 40 and 60 degree	ICC(3,1)	Intra-session: 0.91 (0.81–0.96), CV 7.6%, MDC 9.3, inter-session: 0.66 (0.32–0.84), CV 15.7%, MDC 19.7
Le Sant et al.	2017	Many muscles (MG, LG, SOL, et al.), passive dorsi flexion, icc from 80 % ROM	two-way random ICC	ICC: 0.79-0.97 depending on muscle, CV: 5.3-17.8%
Le Sant et al.	2015	ST, SM, BFlh and BFsh during passive stretch	two-way random intraclass	30% ROM, ICC: 0.71-0.94, SEM 1.1–3.5, CV 10.4–20.3 depending on muscle, higher ICC for ST and SM when more streched, lower for BFlh
Lee et al.	2021	RF, BF, TA, MG, relaxed (and active contraction)	intra-observer, same session	RF:0.916 (0.196–0.994), TA: 0.852 (-0.171–0.992), BF: 0.842 (-0.140–0.989), MG: 0.876 (-0.011–0.991)
Lima et al.	2017	MG (and achiles tendon)	Intra and inter-visit (< 7 days)	Intra, left: 0.982, CV 20.95%, right: 0.986, CV 17.29%, inter: left 0.739, right 0.614
Liu et al.	2021	MG, passive stretch	Intra-observer and inter-observer	Intra-rater: 0.9209 (0.8157–0.9671), inter-rater: 0.9064 (0.7841–0.9609) plantar flexion 25 and biggest ROI
Liu et al.	2020	VL, RF, vastus medialis (VM), sartorius (SAR), gracilis (GRA), BF, ST, SM, GM, and gastrocnemius lateralis (GL), different positions	ICC(3,1)	Ranged from 0.941 to 0.998 (95% CI raged between 0.909–0.999), CV ranged from 1.45% to 9.5%, and SEM 0.026–0.824 kPa
Ma et al.	2020	Back muscles, T3, T7, T11, L1, and L4 sites	Intra- and inter-rater ICC(3,1)	ICC = 0.731–0.881 (95% CI 0.340 to 0.962)
MacDonald et al.	2016	Obliquus externus abdominis, obliquus internus abdominis, transversus abdominis and rectus abdominis, rest (and active)	ICC(3,1) and ICC(3,3)	Intra-session: 0.45–0.89, SEM 0.58–0.99 kPa, CV: 10.2–21.4 %, inter-rater: 0.05–0.89, SEM: 0.49–1.15, CV: 10.4– 27.2, TA being much worse than others
Matsuda et al.	2019	Superficial (and deep) multifidus, 3 positions	ICC1,1	ICCs 0.88, 0.95, and 0.85, (95% CI ranged between 0.57–0.98), SEM 0. –1.24

Authors	Year	Muscles studied	ICC model	Results
Mendes et al.	2018	BFlh and BFsh, ST, SM, 10, 20, 30, 40, 50, 60 % from MVIC	Intra-day ICC(2,1) all contraction levels, inter-day ICC(2,k) only 20 %	0.72–0.93 (95% CI ranged between 0.27–0.98), SEM 3.7–11.4, inter-day 0.69–0.84, 0.27–0.95, SEM 6.41–16.4
Pałac & Linek	2022	Intercostal muscles (and diaphragm)	ICC(3,1)	Intra-rater: 0.85, SEM 1.99, CV 3.18. Inter-session (7 days): 0.50, SEM 4.52, CV 1.04%
Phan et al.	2019	BB and quadriceps muscle in flexion and extension	inter-observer, intra-observer	BBM: intra 0.993 (0.989-0.996), 0.989 (0.982-0.993), inter: 0.976 (0.962-0.985) QM: intra 0.937 (0.896-0.961), 0.886 (0.812-0.931), inter: 0.789 (0.653-0.872)
Saeki et al.	2017	LG, MG, SOL, PL, PB, FHL, FDL, TP s, TP d	ICC(1,3)	Inter-day: 0.58-0.83 depending on muscle, CV .5-12.0%, for 10 and 20 dorsi flexion, the ICC is better
Šarabon et al.	2019	BF passive (and streched - not here)	two-way mixed single	Intra-rater 0.85 (0.71–0.93), intra-rater2 0.74 (0.45–0.88), inter-rater: 0.74 (0.45–0.88), inter-visit 0.34 (0.11–0.67)
Taş et al.	2017	Rectus femoris (RF)	ICC(2,1)	Intra-rater: 0.93 (0.83-0.97), CV 8.7%, SEM 0.18 m/s, inter-rater: 0.95 (0.32-0.88), CV 6.3%, SEM 0.17 m/s, inter-day: 0.81 (0.54-0.92), CV 11.7, SEM 0.24
Vuoren-maa et al.	2022	BB and TA, longi-tudal and trans-verse, relaxed	inter-observer reliability for average meas-urement (and inte-device)	ICC 0.91 (CI 0.88–0.93, SEM 0.63) with scanner 1 and 0.81 (CI 0.74–0.86, SEM 0.76) with scanner 2
Wu et al.	2020	RF, VM, VL, gra-cilis (GRA), BF, ST, SM, GM, GL, relaxed	ICC(3,1) intra-session	ICC 0.952–0.987 (95% CI ranged between 0.923 and 0.992), BF 0.981 (0.966 - 0.984)
Xie et al.	2019	Superficial and deep cervical and axioscapular mus-cles, rest	intra-day ICC(3,1), in-ter-day ICC(3,1), ICC(3, 2) and ICC(3,3) as the number of scans might affect	Superficial intra-session: 0.82, lower bound>0.50 for most superficial muscles, SEM < 1.09 kPa, MDD <3.03 kPa, deep muscles 0.47-0.84, lower bound 0.14-0.67, SEM 0.53-4.69, MDD 1.46-13, **inter-day:** 0.62-0.89, lower bound <0.5 for almost all muscles, SEM values ≤1.78 kPa and MDD values ≤4.92 kPa
Young et al.	2021	Deep posterior cer-vical muscles, prone and seated	ICC(3,k)	Intra-rater: prone: 0.70 (0.31, 0.87), SEM 2.1, MDC 6.0, seated: 0.73 (0.39, 0.90), SEM 2.2, MDC 6.2

As a conclusion from the table 4, the reporting is variable and, for example, ICC has been used in different ways. 95% confidence intervals are not always reported and often the ICC is interpreted without considering the lower bound of the confidence interval. Inter-day reliability seems to be much worse than intra-session reliability, which might be result of the actual stiffness varying between days. Davis et al. (2019) also states in their review article that there is still a large variation in the methods and reporting of the results of SWE studies of the musculoskeletal system. Inter-user reliability has been reported in most studies from good to very good (ICC > 0.6), but large differences in inter-rater reliability have been observed from moderate to very good (ICC > 0.2, ICC > 0.6). The repeatability of measuring tendons seems to be weaker than that of muscles. Inter-day reliability for passive muscle was reported in four studies, in one of which the ICC was 0.33 (poor), in the others ICC > 0.8, i.e. very good. In a recently published study by Sukanen et al. (2023) reliability was reported transparently to point out some aspects of caution with SWE. The reliability (intra-rater and inter-rater) results for triceps surae muscles during passive stretch were poor especially for soleus when interpreting ICC 90 % confidence interval, SEM, CV and MDC all together.

It seems that examining deeper muscles with ultrasound elastography is less reproducible than superficial muscles (Matsuda et al. 2019). For some muscles, different reproducibility results have been obtained (see table 4), which may partly be due to the sensitivity of the method: probe position, pressure, device, and muscle tension affects the results. Therefore, it is probably not meaningful to compare absolute shear modulus values between different studies.

3.3 Shear modulus and other muscle properties

From hamstring muscles, ST has reported to have the lowest passive shear modulus. In a study from Avrillon et al. (2020) SM and BF were 38 % and 42 % stiffer than ST. Miyamoto et al. (2020) found the shear modulus in SM significantly higher than in the BFlh and ST.

When comparing athletes and a group of controls, especially athletes from ice skating, taekwondo, hurdles and football seemed to have lower shear modulus in SM. There were no significant differences in shear modulus values between sexes or the dominant and non-dominant leg. (Avrillon et al. 2020.) Nor did Sukanen et al. (2023) find differences between the sexes, and there were differences in medial gastrocnemius-minus-soleus shear modulus between male gymnasts (smaller than) and basketball players and track and field athletes. On the other hand, McPherson et al. (2020) found higher BFlh stiffness in male than female basketball players.

With gastrocnemius muscle it has been shown that shear modulus values differ along the muscle. In distal parts of the muscle shear modulus values have been systematically higher during a passive stretch. (Le Sant et al. 2017.) Also, Morel et al. (2019) state that SWE measurements do not represent the entire muscle, for example in the case of vastus lateralis (VL). In BFlh the shear wave speed was different along the muscle when knee was flexed, with 20 % from MVIC which is represented in the figure 6 (Miyamoto & Hirata 2021). The results from passive muscles by Miyamoto et al. (2020) are similar: stiffness is higher at the distal site than the proximal site in BFlh, ST and SM.

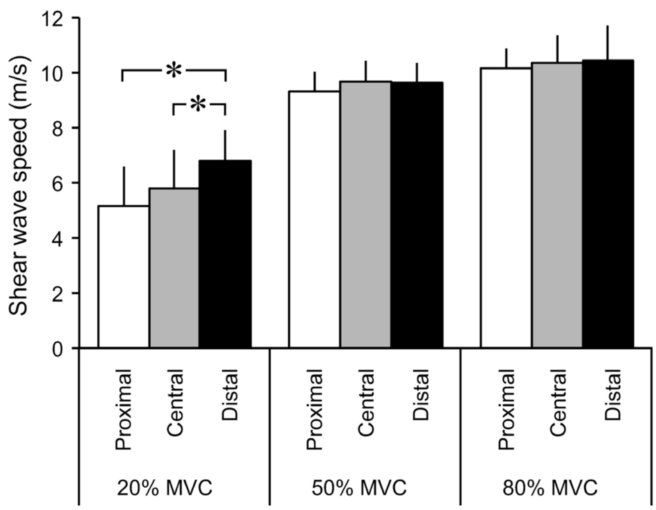

FIGURE 6. SWS in the proximal (white), central (gray), and distal (black) sites of the BFlh at 20%, 50%, and 80% of MVC (Miyamoto & Hirata 2021).

For medial gastrocnemius muscle, it has been reported contradictory results about passive muscle stiffness related to muscle strength. According to Ando & Suzuk (2019) the passive muscle stiffness is not related to force production but according to Yamazaki et al. (2022) high elasticity in passive MG is related to rate of torque development and sprint performance. They also found that stiffness in MG with submaximal contraction correlated with ankle joint stiffness which correlated negatively with 100 meters race time.

Elastic modulus has been found to be linearly related to torque in the abductor digiti minimi (ADM) muscle (Ateş et al. 2015). Bouillard et al. (2012) have also found shear modulus to be linearly related to force output when forces are 0-60% of MVIC. That is, the more the muscle contracts, the stiffer it becomes. However, according to Bernabei et al. (2020), the factors used for combining SWV with Young's modulus do not fully apply to active muscles. The models assume the material is incompressible, isotropic, and homogeneous, which does not apply to muscles. Studies should take into account the behavior of the muscle as a non-linear spring, where the stiffness changes as the force changes, while the muscle length and activation change. However, Bernabei et al. (2020) also consider ultrasound elastography to be a useful additional tool for studying muscle mechanics.

When assessing joint forces and fatigue, possible changes in muscle recruitment should be considered, as joint forces are not caused by a single muscle. Possible changes in the tendon can also affect the geometry of the muscle (Maganaris et al. 2002). Presumably, with a good warm-up, the tendon changes already occur during the warm-up, which reduces the possibility of this error in the studies. In the case of previously mentioned ADM, due to the fusiform structure of the muscle (meaning the fascicles run parallel to the muscle), it can be assumed that the changes were not caused by changes in the pennation angle. (Morel et al. 2019.)

The effects of fatigue on the shear modulus of active and passive muscles have been studied to some extent, but there are some contradictions in the results. After an ultrarunning competition (330 km), Andonian et al. (2016) observed a significant decrease in the shear modulus of the rectus femoris, vastus lateralis and medialis. After an eccentric stiff-leg deadlift exercise the shear modulus of BFlh or ST did not significantly decrease even though it did in SM (Kawama et al. 2022). Freitas et al. (2022) found a decrease in shear modulus of ST but not BFlh after a fatiguing exercise (until exhaustion). During the fatiguing protocol shear modulus behaved differently in football players with a previous hamstring injury than those without.

Following a stretching exercise, shear modulus decreases. In an experiment by Miyamoto et al. (2020) the distal site of the semimembranosus stiffness remained higher compared to the proximal site. The relative change in muscle stiffness was almost the same at the distal and the proximal site. It seems that the highest passive muscle stiffness is not located at the proximal site of the semimembranosus, which is where stretching-type hamstring strains typically occur

(Miyamoto et al. 2020). According to Miyamoto et al (2017), shear modulus decreases significantly in BFlh after knee extension stretching but not after hip flexion maneuver, in ST and SM the decrease is significant after both stretching protocols.

When the muscle-tendon unit (MTU) is stretched, stiffness increases because the surrounding tissues resist this lengthening. How shear modulus changes during passive ankle dorsi flexion or knee extension has been studied in gastrocnemius and hamstring muscles (Lima et al. 2017). In the passive slow joint movement, the muscles lengthen and pennation angle changes. In a study by Le Sant et al. (2015) they found a typical pattern for BFlh during a slow passive knee extension which is illustrated in figure 7. In this study, hip had 110° flexion. According to my current knowledge, it has not been studied how, for example, a different pennation angle or fascicle length between contralateral limb's muscles affect the shear modulus.

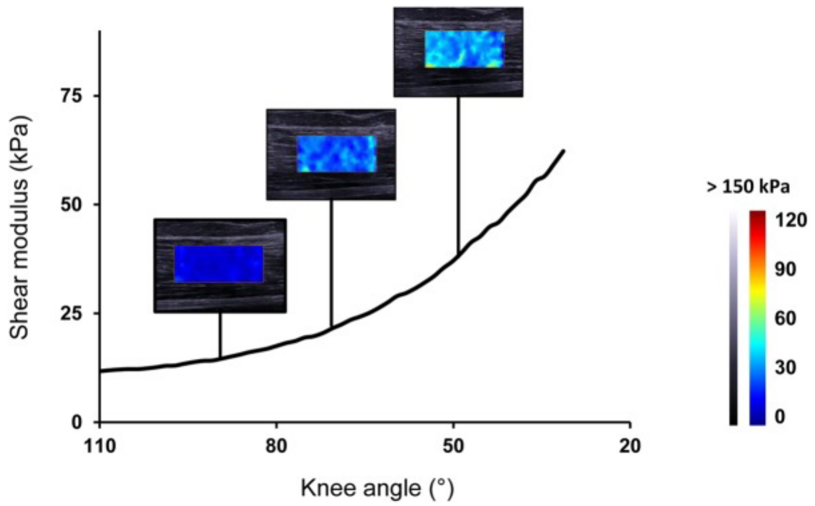

FIGURE 7. Shear modulus-lengthening curve in BFlh (Le Sant et al. 2015).

Based on current knowledge, there are not many studies on the relationship of muscle properties (such as pennation angle and fascicle length) or performance variables to shear modulus measured by SWE. Resting PA has found to positively correlate with fast force production, RFD, in vastus lateralis (Van Hooren et al. 2024). However, according to Blackburn and Pamukoff (2014) hamstring muscle tendon stiffness (measured by damped oscillatory technique) correlates with strength, but PA or fascicle length does not.

According to a review by Sarto et al. (2021) the SWE technique has functional significance as the stiffness being related to force production. Although muscle SWE imaging has its own technical and methodological challenges, the imaging could be useful in monitoring athletes' status, assessing muscle force and mobility of joints and in evaluating and detecting musculoskeletal disorders.

4 PURPOSE OF THE STUDY

The purpose of this thesis study was to investigate SWE imaging on passive BFlh muscle and analyze if the method is reliable. The purpose was also to increase knowledge of the characteristics of BFlh and the connection of these characteristics to performance variables.

1. Are the SWE measurements from relaxed BFlh reliable? (test-retest during same visit)
2. Is the stiffness constant along BFlh? (distal-mid-proximal)
3. Are there relations between muscle thickness/fascicle length/pennation angle and stiffness?
4. Is there relation between BFlh stiffness/(muscle thickness/fascicle length/pennation angle) and strength measured in Nordic hamstring exercise/running performance (30 m sprint)/CMJ and static jump/hamstring:quadriceps ratio?

Hypothesis:

1. Based on previous studies, SWE reliability for BF should be good-excellent (Alfuraih et al. 2018; Lee et al. 2021; Liu et al. 2020).
2. Because the architecture of BFlh varies along the muscle (Timmins et al. 2020), it is assumed that the elasticity measured by SWE is not constant. Yet, the architectural changes are biggest close to the muscle-tendon junctions (Kellis et al. 2010; Tosovic et al. 2016), and here the imaging is done on the muscle belly area.
3. There are connections between architectural properties of muscle (pennation angle and fascicle length) and shear wave speed/tissue stiffness.
4. Performance variables that require high power output are related to stiffer muscle tissue.

Thereby, the aim of the study was therefore to evaluate the usefulness of ultrasound elastography in imaging passive skeletal muscles and to find out which characteristics are related to important performance variables for a football player. Since hamstring injuries are very common and often serious, ultrasound elastography and b-mode imaging may be useful in the future, for example in injury prevention, rehabilitation, or diagnosis.

5 METHODS

The measurements for this thesis were part of a bigger illness and injury monitoring project by the University of Jyväskylä and KIHU (Finnish Institute of High Performance Sport, formerly known as Research Institute for Olympic Sports). All the measurements were done during 2020. Laboratory measurements were done in the Sports and Health laboratories of Jyväskylä University. The research project received a positive statement from the ethics committee of the University of Jyväskylä (5U/2019). Before participating, every participant voluntarily signed a consent form, and they were properly informed about the research contents and the course of the study. It was emphasized to the participants that participation in the study is voluntary, and they have the right to withdraw from the study at any point without it influencing their treatment, for example, within the team.

5.1 Subjects

Subjects of this thesis were female football (soccer) players. All together 42 subjects were measured, from which 31 attended ultrasound measurements and 39 performance tests. 29 attended both sessions. Main characteristics of the 31 subjects attending at least the ultrasound measurements are in the table 5.

TABLE 5. Subject characteristics (N=31).

	Average ± SD
Age	20 years ± 3 years
Height	169 cm ± 6 cm
Weight	66 kg ± 9 kg
BMI	23 ± 2
Total Region %Fat	25 % ± 5 %

5.2 Protocol

The protocol included two different measurement sessions. All of the ultrasound measurements were done during the ”ultrasound session”. This session didn’t include any physical exertion and any vigorous activity was avoided before the measurements on the same day. The performance tests were done during the ”performance session”. Both sessions were performed during football season 2020. DXA-measurement (dual-energy X-ray absorptiometry) and other anthropometrics were measured during a separate visit to the lab, as part of the main monitoring project (between June and October for all participants).

5.2.1 Ultrasound session

All the measurements were done from both legs. Subjects were lying prone on a treatment table, knee extended, and ankle relaxed over the table. First, all the necessary marks were done on the skin using a marker pen: BFlh distal and proximal MTJ (length was measured), middle point between MTJs and six centimeters proximal and distal direction from the middle point, and middle line for the BFlh muscle belly (figure 8).

First, the **panoramic pictures (EFOV)** from BFlh were taken for pennation angle, thickness and fascicle length. At least two panoramic pictures from each leg were saved. The aim was to see the fascicles and swipe the US probe parallel to them from the distal MTJ to the proximal MTJ. The swipes weren’t always following the middle line of the muscle because of the aim for fascicle visibility. For example, Sarto et al. (2021) suggest the use of extended field of view (EFOV) for fascicle length measurements. With traditional US images the extrapolation of the fascicle is a significant limitation.

Second, the **elastography** clips were recorded. For the elastography imaging, a support was set under participants ankles and shins so that the knee angle was 150 degrees, i.e. 30° flexed (as Mendes et al. 2018). The support under subject’s shin had a 30-degree angle, and the knee angle was measured with a goniometer. For both legs there were three different imaging areas: middle point, distal (6 cm) and proximal (6 cm) points as marked in the beginning. These were located in the middle line of the muscle if there weren't big veins or other structures causing void. The ultrasound probe was always positioned as well as possible parallel (longitudinally) to the fascicles as it has been reported to be the most reliable and valid way (for example Liu et al. 2020). From the right leg the measurements were repeated to get data for the intra-session repeatability. All the clips were approximately five seconds long, aiming to have at least three stable elastography frames.

An Aixplorer ultrasound device (version 12.3.1, Supersonic Imagine, Aix-en-Provence, France) was used with a linear SL10-2 array for all the measurements. For the elastography measurements the musculoskeletal (msk) presets were used with couple of changes: optimizing: penetration (because of BFlh being a big muscle), persistance: off, smoothing: 5. Same kind of presets have reported for example Le Sant et al. (2017). With these presets, the elastography frame frequency was 1-1.5 Hz which is automatically adjusted by the device. Ultrasound gel was always used between skin and the probe and minimum possible pressure was applied on the skin.

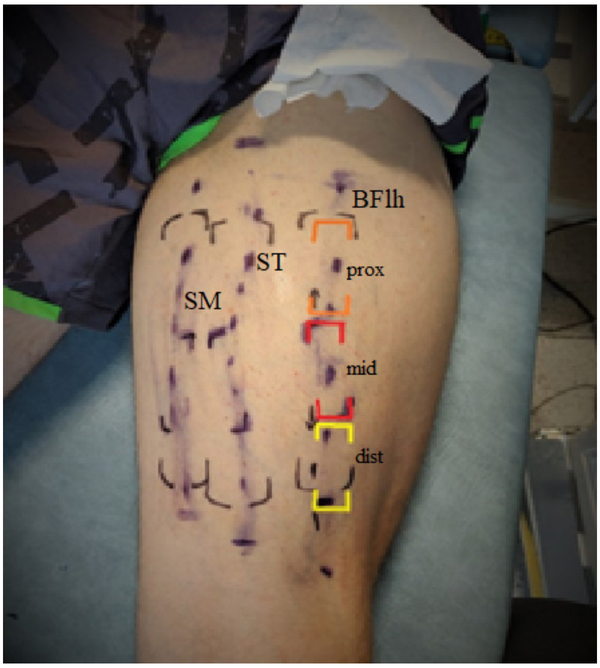

FIGURE 8. Measurement sites for BFlh, the probe placements are marked on the skin. Middle line marks are for EFOV imaging.

5.2.2 Performance session

Standardized warm-up is represented in the table 6.

TABLE 6. Warm-up for the performance tests.

Movement	Duration/reps	Technique	
Indoor cycling	5 min	Own cadence and resistance	
Squat	10	Depth depending on mobility	2x
Knee extension	8 + 8	Lying on back, hip 90°	
One leg hip bridge	5 + 5	Working leg on higher platform	
One leg deadlift	8 + 8	Range depending on mobility	
Reactivity jumps	10	On ball of the feet	

CMJ and static jump. Participants performed two warm-up trials and four test trials of each jump, from which the highest jump was used in the analysis. The jump height was measured using an infrared mat (Spintest, Estonia). Rest intervals between trials were one minute. In both jumps hands were held on hips. In static jump the depth of squat and stop before jumping was controlled by the measurer.

Sprint 30 m. Before the maximum repetitions three submaximal (50 %, 75 % and 90 %) 30 meters were run. Time was measured by photocells (Newtest Oy, Finland) 30 cm from the floor. Participants started 50 cm from the first photocell beam. Rest intervals between the running trials were two minutes.

Nordic hamstring. The position and the measuring device are in the figure 9, force transducers were attached above the ankles. (Hegyi et al. 2019; Opar et al. 2013) The aim was to go as low as possible with the constant speed of 18°/s. (Hegyi et al. 2018.) A metronome was used so that in theory 90° (torso from vertical to horizontal position) would be moved in five seconds. Before the maximum test every participant did test repetition(s) to try the technique and movement velocity. Rest intervals between the trials were three minutes. The force signal was recorded at

1000 Hz and digitized using an A/D converter (Cambridge Electronic Design, Cambridge, UK) and using appropriate software (Spike 2, v6, CED, Cambridge, UK).

FIGURE 9. Nordic hamstring exercise. The same custom-built device was used as in this figure of Hegyi et al. (2018).

Isokinetic force measurements. For the hamstring:quadriceps ratio the isokinetic force measurements were done with a custom-built dynamometer (University of Jyväskylä). The dynamometer allowed a range of motion of 78 degrees: knee angle ranging from 90 to 168 degrees (180 degrees representing full extension). The seat and lever arms were adjusted individually for each participant. The back of the seat was adjusted so that knee joint was at the level of the rotational axis. The lever arm (distance from the rotational axis to the ankle strap with the force sensor) was adjusted depending on the participant's shin length; so that the strap could be comfortably tightened on the proximal side of the malleoli. The length of the lever arm was measured to be used in the analysis. For the smallest participants some extra support behind their back was needed because the seat had limited adjustment possibilities.

For both, knee extensors and flexors, two different speeds (60 and 180 degrees per second) and concentric and eccentric actions were used. Participants conducted four trials for each condition, with a 20-second rest interval between trials. The order of muscle action (concentric or eccentric) was randomized. (As Savolainen et al. 2023.) The highest peak torque for each condition was used for the analyses. The isokinetic force measurements were conducted only on the right leg. Force signal was recorded at 1000 Hz using D/A-converet (CED Power1401-3A, Cambridge, UK) and appropriate software (Spike 2, v6, CED, Cambridge, UK).

For **all the maximum performances** an extra repetition was done if the result improved more than 5 % or if the participant felt like not yet giving the best. All the participants were intensively verbally encouraged during their performances.

Most of the data was collected during summer and autumn of 2020. Due to corona virus pandemic the data collection lasted longer and was not done in the football pre-season phase. In case of four participants the 30 meters sprint results were measured during different measurement session and were approximately six months older than the ultrasound images. Injury or other limitations might have affected their possibility to perform maximal tests during the summer-autumn months.

5.3 Data analysis

Muscle thickness, fascicle length and pennation angles were determined with ImageJ program (1.53k, NIH, USA) from the panoramic pictures. Below in figure 10 is an example of the analysis. The muscle thickness was measured from the middle line (from distal-proximal MTJ) as the perpendicular distance of the aponeuroses. For the fascicle length the segmented line tool was used and a visible as possible fascicle crossing the middle line was chosen and it was followed from the superficial to the deep aponeurosis. The pennation angle was measured with the angle tool between the deep aponeurosis and a fascicle around the same middle region than the measured fascicle and thickness.

FIGURE 10. Muscle thickness, fascicle length, and pennation angle analysis in ImageJ.

Elastography clips were exported as avi-files from the Aixplorer device. The analysis was done using a MATLAB based ElastoGUI software (ElastoGUI, v. R2021b, MathWorks Inc, Natick, MA, USA). A region of interest was drawn as big as possible avoiding void and possible veins or other structures not muscle tissue. From the clip three stable and no-void frames were used to calculate the average values. The ROI was the same for each frame from one clip. An example of ROI is in the figure 11.

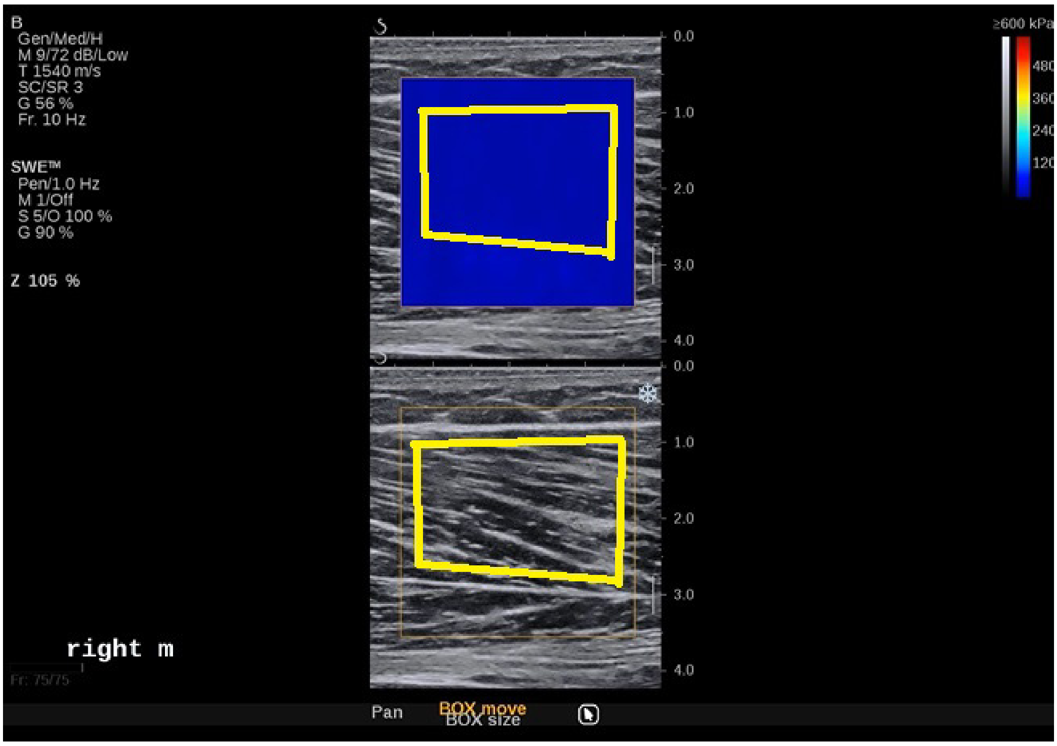

FIGURE 11. Choosing ROI in ElastoGUI.

Force measurements were analyzed in Spike (Spike 2, v6, CED, Cambridge, UK). The maximum force for NHE was determined as the peak force during the best repetition, for both legs separately. This maximum force was divided by the participant's weight. For the isokinetic force measurements, the analysis was also done in Spike and using Excel (Microsoft Excel for Office 365 MSO, Microsoft Corporation, Redmond, Washington, US) spreadsheet. The best repetition with right timing (not starting the force production before movement) was chosen for the analysis. The peak force values were used (the peak force values were considered manually to avoid using interference peaks) checking the peak so that and gravity correction was done using the following equation based on Aagaard et al (1995): $\cos(knee\ angle) \times M_{ref} / \cos 10°$. This correction moment was added (quadriceps) or subtracted (hamstrings) from the original moment $force \times lever\ arm$.

5.4 Statistical analysis

Statistics were done using Excel (Microsoft Excel for Office 365 MSO, Microsoft Corporation, Redmond, Washington, US) and SPSS (IBM SPSS Statistics, version 26.0, IBM Corporation, Armonk, New York, US) programs. Mean ($\bar{x} = \frac{1}{n}\sum_{i=1}^{n} x_i$) and standard deviations ($\sigma = \sqrt{\frac{\sum(x-\bar{x})}{n}}$) were calculate in Excel. All the variables were tested in SPSS if they are normally distributed with Shapiro-Wilks test. Because all the variables were not normally distributed and the results from Pearson and Sperman's rho differed, the Spearman's rho was used. When performing the statistical analysis (except the reliability analysis), the averages of two measurements (if available) were used. P-value smaller than 0.05 was set as a limit of significance for all statistical analysis.

For reliability, ICC was calculated for right legs shear modulus values. ICC describes the strength of correlation and accordance (Koo & Li 2016). According to Davis' et al. (2019) review, the reliability studies of SWE use almost always the ICC (1,1) (*one way random effects, absolute agreement, single measurement*) and/or ICC (2,1) (*two way random effects, absolute agreement, single measurement*), and based on the literature review in this thesis ICC (2,1) and ICC (3,1) are commonly used. The decision should be made depending on the reliability analysis (intra-rater, inter-rater, inter-day etc.). ICC (2,1) is based on the following equation: $\frac{MS\ for\ rows - MS\ for\ error}{MS\ for\ rows + (k-1) \times MS\ for\ error} + \frac{k}{n} \times (MS\ for\ columns - MS\ for\ error)$, where MS is for mean square, k=number of raters/measurements and n=number of subjects (Koo & Li 2016). In their article Koo and Li (2016) describe the use of ICC, and based on this knowledge it is justified to always report the entire ICC table with confidence intervals, although this has not always been the practice in previously published SWE articles. To describe the reliability better CV (coefficient of variation) and SEM (standard error in measurement) were also calculated using SPSS and Excel, as the following equations: $SEM = SD\sqrt{1 - ICC}$ and $CV = SD/mean \times 100\ \%$ (Atkinson & Nevill 1998). MDC (minimal detectable change) or the smallest real difference (SRD) is defined as $MDC = 1.96 \times SEM \times \sqrt{2} \approx 2.77 \times SEM$ (based on Lexell & Downham 2005).

To examine the differences between BFlh imaging sites, the analysis of variance (ANOVA) for repeated measures was done in SPSS (for both legs separately). Depending on the Mauchly's Test of Sphericity, Greenhouse-Geiser with Bonferroni correction or Sphericity Assumed was used for the interpretation. A correlation matrix between the main variables (muscle characteristics and performance) was developed in SPSS, and interpreted as 0.9 to 1.00 very high, 0.70 to 0.90 high, 0.50 to 0.70 moderate, 0.30 to 0.50 low, and 0.00 to 0.30 negligible correlation (Hinkle et al. 2003).

6 RESULTS

Data from every subject measured in the study was used in the analysis and no outliers were excluded. One elastography file from mid BFlh was corrupted and all muscle characteristics didn't have two analyzable images.

6.1 Reliability

ICC values for the SWE measurements are in table 7 showing that the measurements were reliable (moderate-excellent) even if the interpretation is made based on the lower bound of the confidence interval. Based on the ICC value itself, the results are good-excellent. The correlation between the measurements is illustrated in figure 12.

TABLE 7. ICC (2,1) for shear wave values.

INTRA-session		95 % Confidence Interval						
	Intraclass Correlation	Lower Bound	Upper Bound	Sig.	SEM	MDC	CV (%)	N
ALL together	0.854	0.788	0.901	0.000	0.51	1.41	13.1	92
Rdist	0.766	0.572	0.879	0.000	0.75	2.08	16.7	31
Rmid	0.959	0.917	0.980	0.000	0.28	0.78	9.1	30
Rprox	0.869	0.748	0.935	0.000	0.36	1.00	12.4	31

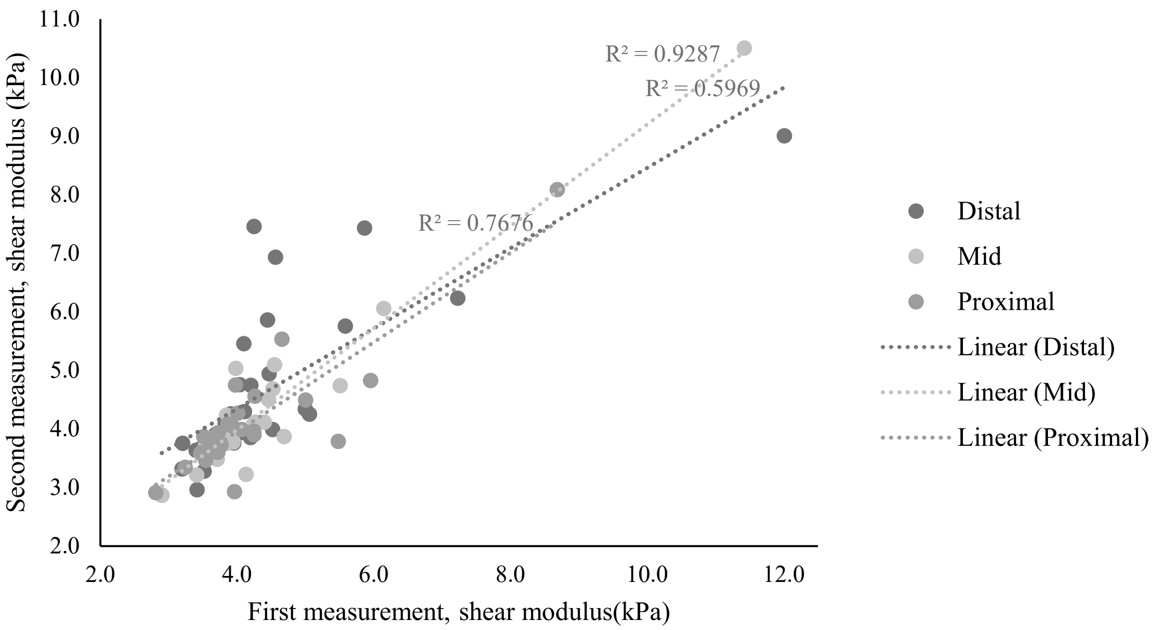

FIGURE 12. Correlation of all the SWE measurements, first and second measurement. The figure illustrates well the worse reliability of distal regions measurements and some exceptional high shear modulus values.

For other muscle characteristics (thickness, fascicle length, pennation angle) the ICC values are summarized in table 8 which shows the reliability being good-excellent (interpreted as Koo & Li 2016).

TABLE 8. ICC analysis for muscle characteristics. Both right and left leg values are used.

INTRA-session	95 % Confidence Interval				
	Intraclass Correlation	Lower Bound	Upper Bound	Sig.	N
Muscle thickness	0.982	0.968	0.990	0.000	49
Fascicle length	0.963	0.934	0.979	0.000	48
Pennation angle	0.935	0.884	0.964	0.000	44

The ICC analysis in table 8 were also performed for the right and left leg separately, but no big differences were observed between them. At most, the lower bound values for the single leg analysis differed by 0.05 from the values in table 8.

6.2 Shear modulus along the muscle and between legs

The average shear modulus values with SD for both legs are presented in the figure 13. Average results of other muscle characteristics for both legs are in the table 9. In paired samples T-test thickness, fascicle length or pennation angle between right and left leg didn't significantly differ from each other.

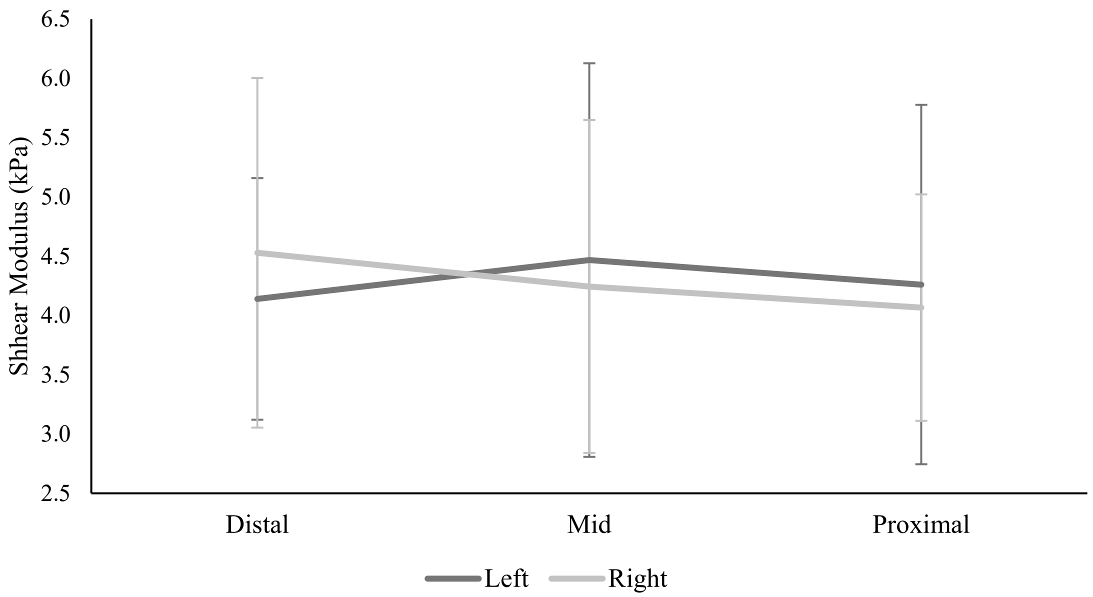

FIGURE 13. Average *shear modulus* values for right and left BFlh in distal, mid, and proximal measurement sites (± SD).

TABLE 9. Muscle characteristics, averages with SD.

	Muscle thickness (cm)	SD	Fascicle length (cm)	SD	Pennation angle (°)	SD	Muscle mass, leg (kg)	SD	n
Right leg	2.33	0.28	9.93	1.97	14.0	2.0	8.0	1.2	31
Left leg	2.24	0.35	9.23	1.62	14.0	2.6	7.9	1.1	31
Difference	0.09		0.70		0		0.1		

Repeated measures ANOVA showed no difference between the mean value of three different measurement sites in the left leg (dist=4.1399, mid=4.4678, prox=4.2613, p=0.226, Greenhouse-Geiser). In the right leg the test showed significant difference between the imaging sites (dist=4.485, mid=4.245, and prox=4.057, p=0,017, Spherity assumed). In pairwise comparison, there was difference between shear modulus in distal and proximal sites (p=0.047). The figure 14 shows individual shear modulus values in the different imaging sites in right and left leg separately.

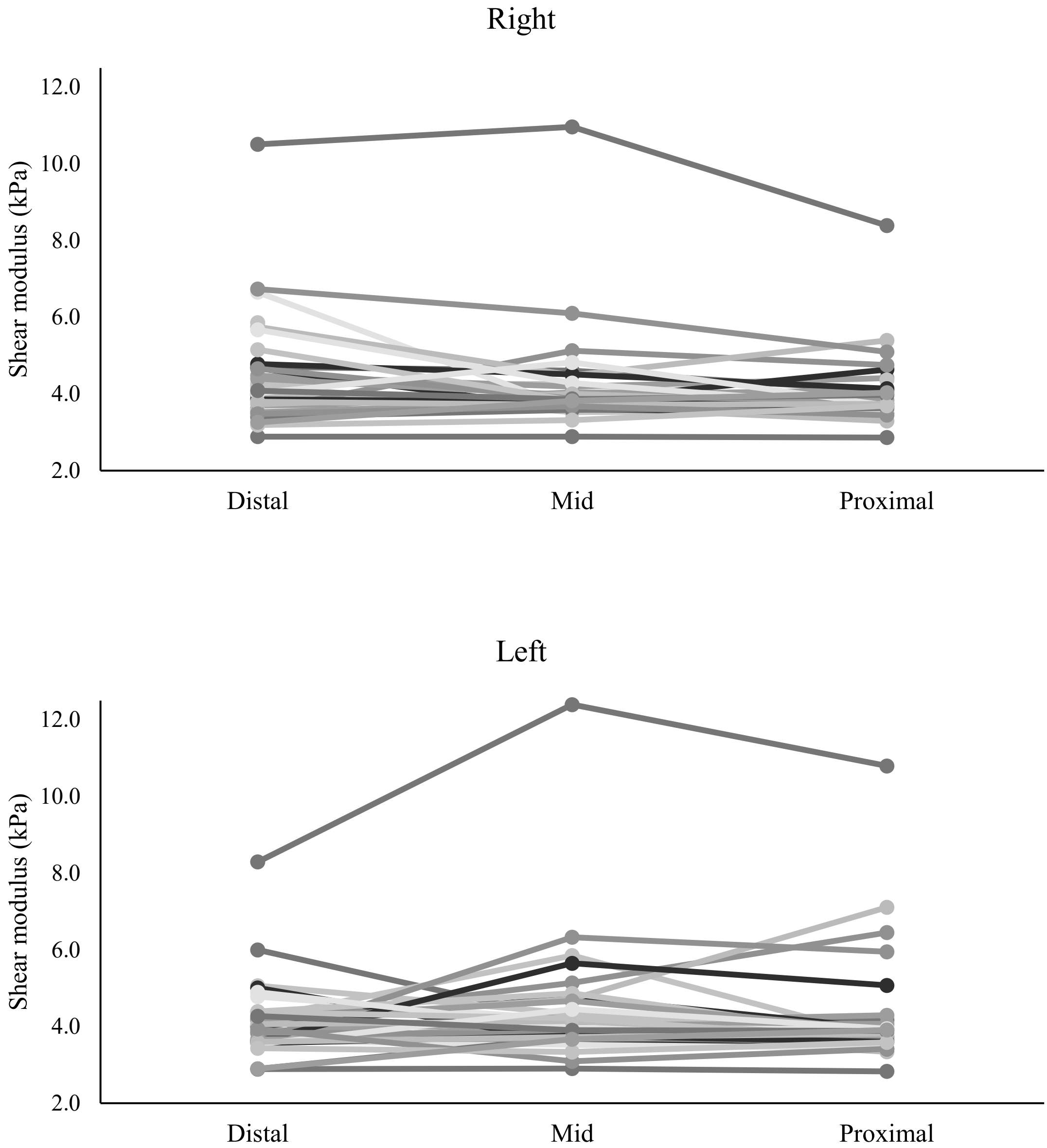

FIGURE 14. Shear modulus in distal, mid and proximal imaging site individually for each participant. Upper for right leg and lower for left. The exceptional values in both legs are from the same participant.

Individually there were no significant differences in shear modulus between right and left leg when using the averaged value (paired samples test, p=0.972). In distal and mid imaging sites there were statistical differences between legs but not in proximal, see table 10.

TABLE 10. Differences in shear modulus between legs.

	Mean difference	Lower	Upper	p-value
Left distal – right distal	-0.39	-0.73	-0.05	0.026
Left mid – right mid	0.21	0.01	0.41	0.038
Left proximal – right proximal	0.19	-0.05	0.44	0.114
Left average – right average	0.00	-0.16	0.16	0.972

6.3 Other muscle characteristics and average stiffness

Correlation matrix for muscle thickness, fascicle length, pennation angle, shear modulus (average from all three measurement sites and both legs), leg lean mass based on DXA measurement and Nordic hamstring exercise peak force for one leg is presented in table 11. Right and left leg are both used for this analysis (N=55-62, depending on the variable). Shear modulus from both legs seemed to correlate with height (0.431, p=0.015 left and 0.444, p=0.012 right). There were also significant correlations between right and left leg thickness (0.667, p=0.000), fascicle length (0.788, p=0.000) and pennation angle (0.526, p=0.002).

TABLE 11. Correlation (non-parametric Spearman's) matrix between muscle characteristics and shear modulus (average form distal, mid and proximal sites). Data from both legs is used, *p < 0.05, **p > 0.01.

	Muscle thickness	Fascicle length	Pennation angle	Average shear modulus	Lean mass, leg
Muscle thickness	1	**0.437****	0.224	0.179	**0.329****
sig.		**0.000**	0.080	0.164	**0.000**
Fascicle length		1	-0.470**	-0.142	**0.394****
sig.			0.000	0.270	**0.002**
Pennation angle			1	**0.267***	-0.062
sig.				**0.036**	0.632
Average shear modulus				1	0.179
sig.					0.167

6.4 Muscle characteristics and performance

The average performance results and SD are in table 12, which provide more information about the participant group's characteristic.

TABLE 12. Average results for the performance variables.

	Result	SD	n
30 m (s)	4.68	0.16	30
CMJ (cm)	31.2	3.2	30
Static jump (cm)	29.8	3.2	30
NHE, F/mass	1.14	0.22	28
Hecc60/Qcon60	0.72	0.40	28
Hecc180/Qcon180	1.07	0.61	28
Hcon60/Qcon60	0.50	0.22	28
Hcon180/QCon180	0.58	0.23	28

The main muscle characteristics and anthropometric variables and their correlations with the performance variables are presented in table 13. Shear modulus correlated significantly with 30 meters time and lean mass of the legs with jump performance and NHE. Muscle thickness did not correlate to any performance variable and is not visible in the table. NHE max force divided by participant's mass did not correlate to any muscle or anthropometric variables.

TABLE 13. Muscle characteristics and performance variables. Spearman's rho, correlation co-efficient. Shear modulus abbreviated as sm. *Correlation is significant at the 0.05 level, **correlation is significant at the 0.01 level (2-tailed).

	30 m sprint	CMJ	Static jump	NHE right	NHE left	Hecc60/ Qcon60	Hecc180/ Qcon180	Hcon60/ Qcon60	Hcon180/ QCon180
R FL	-0.30	**,379***	**,441***	0.28	**,414***	0.06	0.33	0.11	0.19
R PA	0.10	-0.27	-0.07	0.01	-0.10	-0.04	**-,407***	-0.10	-0.08
L FL	-0.23	0.33	0.32	0.03	0.08	0.04	0.30	-0.05	-0.04
L PA	0.00	-0.09	-0.16	0.19	0.04	-0.15	**-,392***	-0.11	-0.05
Avg. LEFT sm	**,471****	-0.20	-0.21	0.11	0.11	0.02	0.05	-0.12	-0.03
Avg. RIGHT sm	**,387***	-0.03	-0.10	0.20	0.17	-0.08	-0.11	-0.23	-0.06
Avg. R + L sm	**,450***	-0.09	-0.15	0.15	0.13	-0.03	-0.03	-0.18	-0.06
Leg Right Lean Mass	-0.23	**,572****	**,634****	**,596****	**,620****	0.04	0.22	0.00	0.09
Leg Left Lean Mass	-0.22	**,584****	**,595****	**,613****	**,599****	0.03	0.18	-0.01	0.05
Legs lean mass	-0.25	**,587****	**,633****	**,617****	**,622****	0.06	0.21	0.01	0.08
Total Region %Fat	0.33	-0.22	-0.19	0.09	0.11	-0.22	-0.02	-0.27	-0.11

7 DISCUSSION

The overall reliability of SWE, PA, FL and MT measurements was good to excellent. Shear modulus along the BFlh muscle had some statistically significant differences in right but not in left leg. Generally, there were no high correlations between other muscle characteristics and shear modulus, or muscle characteristic and shear modulus and performance variables. Some statistically significant moderate and low correlations were found; shear modulus with 30 meters time, lean mass with jump performance and NHE force, as examples.

As said, the reliability of SWE measurements was good to excellent. Interestingly SWE from the mid part of BFlh showed excellent reliability and from the more distal region poor to good reliability (interpreted as Koo & Li 2016). The results are in line with most of the previous studies where the reported ICCs vary but are often reported to be good-excellent for muscles (see table 4), and for example Šarabon et al. (2019) reported relaxed BFlh intra-rater ICC 0.85 (95 % CI 0.71–0.93) and for another measurer 0.74 (0.45–0.88). According to Koo and Li (2016), reliability should be classified based on the 95% confidence interval, as the actual ICC can be anywhere between the lower and upper limits. Based on the values of the confidence interval, the reliability is said to be poor (< 0.5), moderate (0.5-0.75), good (0.75-0.9) or excellent (excellent > 0.90). On the other hand, for example, Baumer et al. (2017) use the following interpretation in their reliability study, referring to Altman (1991): 0-0.2 bad, 0.21-0.4 moderate (fair), 0.41-0.6 reasonable (moderate), 0.61-0.8 good and 0.81-1.00 very good, and report only the actual ICC without the confidence intervals. Joo et al. (2019) use also the same limits in slightly different terms (0.61-0.80 strong and > 0.80 excellent) and classify according to the actual ICC value. However, the 95% confidence intervals of the ICC are reported. For example, Rosskopf et al. (2016) report good reliability with ICC = 0.70, 95% CI: 0.30-0.87, p = 0.003 and excellent with ICC = 0, 80, 95% CI: 0.53-0.92, p = 0.001, i.e. according to the actual ICC value.

CV (9.1-16.7 %) is also similar to what has been published (for example 15.3 % for vastus lateralis Bravo-Sánchez et al. 2021; for rectus femoris CV 8.7 % Taş et al. 2017; for abdominal muscles CV 10.2-21.4 % MacDonald et al. 2016). SEM (0.28-0.75 kPa) and MDC (0.78-2.08

kPa) seem to be in line with some previous studies (Liu et al. 2020; different muscles and positions, SEM 0.026-0.824 kPa) or better (Bravo-Sánchez et al. 2021: relaxed vastus lateralis SEM 5.60 kPa; Kozinc & Šarabon 2021: relaxed trapezius 9.3 kPa). Although many SWE studies have been published recently, there are still limited studies on the biceps femoris. Inter-session reliability wasn't studied in this thesis, but it would give much more information about the usefulness of SWE in screening. For studying inter-day reliability, the previous physical activity needs to be well controlled and the landmarks for the measurement precisely specified.

The muscle architecture measurements (pennation angle, thickness and fascicle length) and analysis showed good to excellent reliability as would be expected based on the previous literature. Pennation angle was the only variable not having excellent reliability. In a study by Tosovic et al. (2016), pennation angle had worse reliability than other muscle characteristics. The average thickness 2.33 cm (0.28 cm), fascicle length 9.93 cm (1.97 cm) and pennation angle 14° (2.0°) are in line with those reported by Tosovic et al. (2016) in male participants, 36.4 mm (5.7), 82.7 mm (12.7) and 13.9° (2.8) respectively. Contrary to expectations, fascicle length seems to be smaller in Tosovic et al. (2016) which may be due to the segmented line (versus straight line by Tosovic) analysis tool used in this thesis. In this thesis the reliability analysis was greatly affected by analysis. The analysis wasn't done blinded and the US images from same participant were analyzed in a row. This probably increases the reliability but in this way the focus is on the repeated scan (if it gives the same result) and not so much on the analysis (if the analysis method is reliable). To use these variables in an intervention study, an inter-session reliability analysis would be needed.

The average shear modulus (mid site, both legs 4.36 kPa, SD 1.5 kPa) was lower than in for example Šarabon et al. (2019) reported (17.49 kPa SD 5.18) but they didn't report the exact position of hip and knee. The mean shear modulus was 7.59 kPa with knee in 90° in an article by Alfuraih et al. (2017). These results are in line with the average results of this thesis when the muscle length (knee angle) is taken into account. The backgrounds of the participants may also affect the results, as, for example, the shear modulus values of the passive SM have been found to be lower in athletes in sports that include wide ranges of motion (Avrillon et al. 2020).

The results show that there was a significant difference in the shear modulus between the imaging sites in right but not in left leg. By interpreting the figure 14 it looks like the differences are participant-specific and as expected, the differences between participants are greater than between imaging sites. Miyamoto et al. (2020) found that the shear modulus of BFlh (and SM and ST) is higher at the distal than the proximal site. However, in this study the muscle length was different, as the hip was flexed to 90 degrees and two different knee angles were used. Also, the imaging sites were different, as they were defined as percentages (25 %, 50 % and 75 %) of the muscle belly length.

Results between legs seem to be quite similar and the standard deviation is big. There was a significant difference between legs in distal site showing lower shear modulus in the left leg. As the dominant leg (right) being the kicking leg for all the study participants, the load on hamstrings and other muscles on the limbs is different between the legs. Unfortunately, the isokinetic strength testing was only done on right leg. Significant correlations between right and left leg thickness, fascicle length, and pennation angle were found as expected. Also, muscle thickness and fascicle length had weak but significant correlation with each other, as well as these variables with lean mass of leg. The only performance variable which correlated significantly (low correlation) with shear modulus values was the 30 meters sprint time, meaning negative influence of higher shear modulus. These results aren't in line with the finding by Blackburn and Pamukoff (2014), that hamstring muscle tendon stiffness (measured by damped oscillatory technique) correlates with strength. It should of course be noted, that the muscle tendon stiffness isn't the same as the muscle tissue stiffness (shear modulus) measured in this study but it would be interesting to compare these more.

Muscle lean mass in leg (from DXA imaging) correlated significantly with MT and FL (0.329 and 0.394, p=0.000) and so did MT with FL (0.437, p=0.000) as would be expected. Even higher positive correlations could have been expected. Average shear modulus had a negligible correlation with pennation angle (0.267, p=0.036). Because the fascicle orientation has been reported to have significant effects on shear modulus values, also this correlation could have hypothesized being higher. From these results it can be interpreted that shear modulus in BFlh is highly participant specific and other tissue characteristics (than measured here) affect it more.

Between PA, FL, MT and performance variables there were some low correlations. Pennation angle from both legs had a negative low correlation with Hecc180/Qcon180 results. FL from right leg correlated (low) with CMJ, static jump and NHE left. Muscle thickness did not correlate with any of the performance variables. These results should be interpreted with caution, as the results were not the same in both legs and there is no clear explanatory factor. Lean mass in legs was correlated with CMJ, static jump and force measured in Nordic hamstring exercise. For example, Temfemo et al. (2008) have found significant correlations between leg muscle volume and lean body mass with power output in CMJ and static squat jump in adolescent boys and girls. Van Hooren et al. (2024) found positive correlation between resting PA and fast force production, RFD, in vastus lateralis but similar results were not found in this study. Correlation between leg lean mass and NHE max force was as expected; more mass with ability to product force.

There are many limitations in the study. Shear wave elastography clips were exported from Aixplorer device in AVI-format. After exporting the clips, the most accurate pixel by pixel qualitative data is lost. The clips include the frames with the color maps and ElastoGUI interprets the colors. For this analysis approach a more precise choice for the elasticity range should have been made. At first, the analysis was intended to do in the Aixplorer device where the quantitative data is stored but the plan was changed because of large amount of data and long data collection period (free hard drive space in the Aixplorer needed) and the possibility of ElastoGUI use. Also, ElastoGUI (for example Le Sant et al. 2017; Sukanen et al. 2023) or other Matlab based software (for example Siracusa et al. 2019; Taş et al. 2017; Tier et al. 2021) are often used in elastography analysis. A comparison study between the results analyzed by ElastoGUI and Aixplorer and comparing different elasticity ranges during the acquisition should be done to make the results more generalizable.

In this thesis ROI size in SWE was big and it covered the whole muscle area (rarely in SWE studies), fascicles were oriented well in line with the probe and the muscle was relaxed. As these are the main factors contributing variance (Ruby et al. 2019), the good reliability results were expected. Depth of the SWE imaging was depended on the thigh structure: thickness of the subcutaneous tissue and BFlh muscle itself. According to Ruby et al. (2019) the signal-to-noise ratio of shear wave measurements decreases when imaging deeper structures which has an effect on the accuracy of shear wave imaging. All the ultrasound imaging, especially the SWE, was done with minimum pressure and with gel between the probe and participant's skin. Still, the pressure may vary between repetitions and the SWE is remarkable sensitive to pressure (Pimenta et al. 2024; Taljanovic et al. 2017; Wang et al. 2020). Also, one aspect of the SWE imaging is the muscle tension by the participant as the tension significantly increases the shear modulus (Ruby et al. 2019). One participant had especially high shear modulus values. There was nothing special in the measurement session or the US clips and images. One explanation may be that the muscle was contracted a bit for some reason. The values of this exceptional participant were left in the analysis because everything seemed normal in the protocol and the elastography clips. The tension of the muscle could have been controlled with s-EMG.

The participants of this study were young female football players. The results are not necessarily generalizable to male – females have usually thicker subcutaneous tissue especially in lower limbs and as said, the imaging depth may affect the SWS (Ruby et al 2019). As one limitation of this study, participants' previous exercise may have affected the results, despite the instructions (no physical exercise during the measurement day). Strenuous exercise before the SWE measurements could influence the shear modulus (Andonian et al. 2016; Morel et al. 2019; Siracusa et al. 2019). A light warm-up before the SWE measurements could reduce the effects of previous activity, and this would be important especially in a follow-up or intervention study.

Due to the coronavirus pandemic the data collection period was long and time between different measurements grew long and could not be controlled. Ideally, the ultrasound session, all the performance tests and DXA imaging would have been during the same week and in the preseason phase. Now there might have been essential changes in muscle characteristics, anthropometrics and even in maximal performance.

At least the following things have probably caused some error in the performance variables: lever arm measurement, seat positioning and performance technique (especially in fast concentric) in isokinetic force, different squat depths in static jump, deficiencies in core strength and uneven position on Nordic hamstring exercise. To understand better hamstring stiffness and functioning, SWE could be imagined from SM and ST also, and EMG activity along these three muscles could be measured by HD-EMG during exercises. By this, more individual activation and stiffness patterns could be created, knowledge of muscle function and common areas of injury could be increased. Later, this could be useful in the prevention, treatment, and more accurate diagnosis of injuries. In future studies SWE imaging sites along muscles could be more separated to find out the differences between muscle belly versus close to muscle-tendon junction areas. In future studies the protocols should be carefully designed, taking into account all sources of error. SWE analysis methods could be further developed to make the analysis more precise, objective and still easy to perform.

As a strength, this study had a good number of reliability data for ICC analysis (often for SWE only 10-15 (for example Baumer et al. 2017; Blain et al. 2018; Mendes et al. 2018). In addition, many variables were measured, and data combined. Up to date and knowledge, there aren't studies that have examined hamstring muscle structure and SWE and linked this information to performance variables. In the future, it would be interesting to study the relationships between the properties of several lower limb muscles, including shear modulus, and performance variables. This might give some explanations of the relations of these muscle characteristics with, for example, running performance, which is a multi-joint movement and requires fast force production.

According to Blackburn and Pamukoff (2014) stiffer hamstrings (musculotendinous) might be associated with fewer ACL injuries and vice versa. Since ACL injuries are very common and require a lot of absences especially in female football (Waldén et al. 2011), their prevention, in addition to hamstring injuries themselves, is essential. SWE could be potential technique to monitor injury prevention and rehabilitation programs. Based on the isokinetic tests (Hcon:Qcon 60 °/s 0.72, Hecc:Qcon 60 °/s 0.50), also participants of this study are at increased risk of injury (Baroni et al. 2020: Hcon:Qcon should be over 60 %, Hecc:Qcon 60 °/s should be around 80 %). Some of the participants had history of ACL injuries but their data were processed as any other.

As a conclusion of this study, the SWE and muscle architectural measurement from biceps femoris long head were reliable. Shear modulus wasn’t constant along BFlh but statistically significant differences were only between distal and proximal sites in right leg only. Only some low-to-moderate correlations were found between muscle characteristic and performance.

REFERENCES

Aagaard, P., Simonsen, E. B., Trolle, M., Bangsbo, J., & Klausen, K. 1995. Isokinetic hamstring/quadriceps strength ratio: influence from joint angular velocity, gravity correction and contraction mode. Acta physiologica Scandinavica, 154(4), 421–427. https://doi.org/10.1111/j.1748-1716.1995.tb09927.x

Ahmad, C. S., Redler, L. H., Ciccotti, M. G., Maffulli, N., Longo, U. G., & Bradley, J. 2013. Evaluation and management of hamstring injuries. The American journal of sports medicine, 41(12), 2933–2947. https://doi.org/10.1177/0363546513487063

Al Attar, W.S.A., Soomro, N., Sinclair, P.J. et al. 2017. Effect of Injury Prevention Programs that Include the Nordic Hamstring Exercise on Hamstring Injury Rates in Soccer Players: A Systematic Review and Meta-Analysis. Sports Med 47, 907–916. https://doi.org/10.1007/s40279-016-0638-2

Alfuraih, A. M., O'Connor, P., Hensor, E., Tan, A. L., Emery, P., & Wakefield, R. J. 2018. The effect of unit, depth, and probe load on the reliability of muscle shear wave elastography: Variables affecting reliability of SWE. Journal of clinical ultrasound : JCU, 46(2), 108–115. https://doi.org/10.1002/jcu.22534

Alfuraih, A. M., O'Connor, P., Tan, A. L., Hensor, E., Emery, P., & Wakefield, R. J. 2017. An investigation into the variability between different shear wave elastography systems in muscle. Medical ultrasonography, 19(4), 392–400. https://doi.org/10.11152/mu-1113

Ando, R., & Suzuki, Y. 2019. Positive relationship between passive muscle stiffness and rapid force production. Human movement science, 66, 285–291. https://doi.org/10.1016/j.humov.2019.05.002

Andonian, P., Viallon, M., Le Goff, C., de Bourguignon, C., Tourel, C., Morel, J., Giardini, G., Gergelé, L., Millet, G. P., & Croisille, P. (2016). Shear-Wave Elastography Assessments of Quadriceps Stiffness Changes prior to, during and after Prolonged Exercise: A Longitudinal Study during an Extreme Mountain Ultra-Marathon. PloS one, 11(8), e0161855. https://doi.org/10.1371/journal.pone.0161855

Andrade, M. S., Junqueira, M. S., Andre Barbosa De Lira, C., Vancini, R. L., Seffrin, A., Nikolaidis, P. T., Rosemann, T., & Knechtle, B. 2021. Age-related differences in torque in angle-specific and peak torque hamstring to quadriceps ratios in female soccer players from 11 to 18 years old: A Cross-sectional study. Research in sports medicine (Print), 29(1), 77–89. https://doi.org/10.1080/15438627.2020.1742713

Askling, C. M., Tengvar, M., Saartok, T., & Thorstensson, A. 2007a. Acute first-time hamstring strains during high-speed running: a longitudinal study including clinical and magnetic resonance imaging findings. The American journal of sports medicine, 35(2), 197–206. https://doi.org/10.1177/0363546506294679

Askling, C. M., Tengvar, M., Saartok, T. & Thorstensson, A. 2007b. Acute First-Time Hamstring Strains during Slow-Speed Stretching. Clinical, Magnetic Resonance Imaging, and Recovery Characteristics 35 (10), 1716-1724. https://doi.org/10.1177/0363546507303563

Ateş, F., Hug, F., Bouillard, K., Jubeau, M., Frappart, T., Couadec, M., Bercoff, J. & Nordez, A. 2015. Muscle shear elastic modulus is linearly related to muscle torque over the entire range of isometric contraction intensity. Journal of Electromyography and Kinesiology 25 (4), 703-708. https://doi.org/10.1016/j.jelekin.2015.02.005

Atkinson, G., & Nevill, A. M. 1998. Statistical methods for assessing measurement error (reliability) in variables relevant to sports medicine. Sports medicine (Auckland, N.Z.), 26(4), 217–238. https://doi.org/10.2165/00007256-199826040-00002

Avrillon, S., Hug, F. & Guilhem, G. 2018. Between-muscle differences in coactivation assessed using elastography. Journal of Electromyography and Kinesiology 43, 88-94. https://doi.org/10.1016/j.jelekin.2018.09.007

Avrillon, S., Lacourpaille, L., Hug, F., Le Sant, G., Frey, A., Nordez, A. & Guilhem, G. 2020. Hamstring muscle elasticity differs in specialized high-performance athletes. Scandinavian Journal of Medicine & Science in Sports 30 (1), 83–91. https://doi.org/10.1111/sms.13564

Baroni, B. M., Ruas, C. V., Ribeiro-Alvares, J. B., & Pinto, R. S. 2020. Hamstring-to-Quadriceps Torque Ratios of Professional Male Soccer Players: A Systematic Review. Journal of strength and conditioning research, 34(1), 281–293. https://doi.org/10.1519/JSC.0000000000002609

Baumer, T. G., Davis, L., Dischler, J., Siegal, D. S., van Holsbeeck, M., Moutzouros, V., & Bey, M. J. 2017. Shear wave elastography of the supraspinatus muscle and tendon: Repeatability and preliminary findings. Journal of biomechanics, 53, 201–204. https://doi.org/10.1016/j.jbiomech.2017.01.008

Bedewi, M. A., Alhariqi, B. A., Aldossary, N. M., Gaballah, A. H., & Sandougah, K. J. 2021. Shear wave elastography of the scalene muscles in healthy adults: A preliminary study. Medicine, 100(32), e26891. https://doi.org/10.1097/MD.0000000000026891

Bernabei, M., Lee, S. S. M., Perreault, E. J. & Sandercock, T. G. 2020. Shear wave velocity is sensitive to changes in muscle stiffness that occur independently from changes in force. Journal of Applied Physiology 128 (1), 8–16. https://doi.org/10.1152/japplphysiol.00112.2019

Blackburn, J. T., & Pamukoff, D. N. 2014. Geometric and architectural contributions to hamstring musculotendinous stiffness. Clinical biomechanics (Bristol, Avon), 29(1), 105–110. https://doi.org/10.1016/j.clinbiomech.2013.10.011

Blain, M., Bedretdinova, D., Bellin, M. F., Rocher, L., Gagey, O., Soubeyrand, M., & Creze, M. 2019. Influence of thoracolumbar fascia stretching on lumbar back muscle stiffness: A supersonic shear wave elastography approach. Clinical anatomy (New York, N.Y.), 32(1), 73–80. https://doi.org/10.1002/ca.23266

Bouillard, K., Hug, F., Guével, A. & Nordez, A. 2012. Shear elastic modulus can be used to estimate an index of individual muscle force during a submaximal isometric fatiguing contraction. Journal of Applied Physiology 113 (9), 10.1152. https://doi.org/10.1152/japplphysiol.00858.2012

Bravo-Sánchez, A., Abián, P., Sánchez-Infante, J., Esteban-Gacía, P., Jiménez, F., & Abián-Vicén, J. 2021. Objective Assessment of Regional Stiffness in Vastus Lateralis with Different Measurement Methods: A Reliability Study. Sensors (Basel, Switzerland), 21(9), 3213. https://doi.org/10.3390/s21093213

Brockett, C. L., Morgan, D. L., & Proske, U. 2001. Human hamstring muscles adapt to eccentric exercise by changing optimum length. Medicine and science in sports and exercise, 33(5), 783–790. https://doi.org/10.1097/00005768-200105000-00017

Chino, K., Akagi, R., Dohi, M., Fukashiro, S., & Takahashi, H. 2012. Reliability and validity of quantifying absolute muscle hardness using ultrasound elastography. PloS one, 7(9), e45764. https://doi.org/10.1371/journal.pone.0045764

Chino, K., Kawakami, Y., & Takahashi, H. 2017. Tissue elasticity of in vivo skeletal muscles measured in the transverse and longitudinal planes using shear wave elastography. Clinical physiology and functional imaging, 37(4), 394–399. https://doi.org/10.1111/cpf.12315

Creze, M., Bedretdinova, D., Soubeyrand, M., Rocher, L., Gennisson, J. L., Gagey, O., Maître, X., & Bellin, M. F. 2019. Posture-related stiffness mapping of paraspinal muscles. Journal of anatomy, 234(6), 787–799. https://doi.org/10.1111/joa.12978

Cui, X. W., Li, K. N., Yi, A. J., Wang, B., Wei, Q., Wu, G. G., & Dietrich, C. F. (2022). Ultrasound elastography. Endoscopic ultrasound, 11(4), 252–274. https://doi.org/10.4103/EUS-D-21-00151

Davis, L. C., Baumer, T. G., Bey, M. J. & van Holsbeeck, M. 2019. Clinical utilization of shear wave elastography in the musculoskeletal. Ultrasonography 38 (1), 2–12. https://doi.org/10.14366/usg.18039

De Ste Croix, M., Priestley, A., Lloyd, R., & Oliver, J. 2018. Age-Related Differences in Functional Hamstring/Quadriceps Ratio Following Soccer Exercise in Female Youth Players: An Injury Risk Factor. Pediatric exercise science, 30(3), 376–382. https://doi.org/10.1123/pes.2017-0034

Ditroilo, M., De Vito, G., & Delahunt, E. 2013. Kinematic and electromyographic analysis of the Nordic Hamstring Exercise. Journal of electromyography and kinesiology: official journal of the International Society of Electrophysiological Kinesiology, 23(5), 1111–1118. https://doi.org/10.1016/j.jelekin.2013.05.008

Dubois, G., Kheireddine, W., Vergari, C., Bonneau, D., Thoreux, P., Rouch, P., Tanter, M., Gennisson, J. L., & Skalli, W. 2015. Reliable protocol for shear wave elastography of lower limb muscles at rest and during passive stretching. Ultrasound in medicine & biology, 41(9), 2284–2291. https://doi.org/10.1016/j.ultrasmedbio.2015.04.020

Dulgheriu, I. T., Solomon, C., Muntean, D. D., Petea-Balea, R., Lenghel, M., Ciurea, A. I., & Dudea, S. M. 2022. Shear-Wave Elastography and Viscosity PLUS for the Assessment of Peripheric Muscles in Healthy Subjects: A Pre- and Post-Contraction Study. Diagnostics (Basel, Switzerland), 12(9), 2138. https://doi.org/10.3390/diagnostics12092138

Dvorak J., Junge A., Derman W., & Schwellnus M. 2011. lnjuries and illnesses of football players during the 2010 FIFA World Cup. British Journal of Sports Medicine 45 (8), 626-630. https://doi.org/10.1136/bjsm.2010.079905

Eby, S. F., Song, P., Chen, S., Chen, Q., Greenleaf, J. F., & An, K. N. 2013. Validation of shear wave elastography in skeletal muscle. Journal of biomechanics, 46(14), 2381–2387. https://doi.org/10.1016/j.jbiomech.2013.07.033

Ekstrand, J., Healy, J. C., Waldén, M., Lee, J. C., English, B. & Hägglund, M. 2012. Hamstring muscle injuries in professional football: the correlation of MRI findings with return to play, British Journal of Sports Medicine 46 (2), 112-7. https://doi.org/10.1136/bjsports-2011-090155

Ekstrand, J., Hägglund, M., Kristenson, K., Magnusson, H. & Waldén, M. 2013. Fewer ligament injuries but no preventive effect on muscle injuries and severe injuries: an 1I-year follow-up of the UEFA Champions League injury study. British Journal of Sports Medicine 47 (12), 732-7. https://doi.org/10.1136/bjsports-2013-092394

Erickson, L. N. & Sherry, M. A. 2017. Rehabilitation and return to sport after hamstring strain injury. Journal of Sport and Health Science 6 (3), 262–270. https://doi.org/10.1016/j.jshs.2017.04.001

Eustace, S. J., Page, R. M., & Greig, M. 2019. Isokinetic strength differences between elite senior and youth female soccer players identifies training requirements. Physical therapy in sport : official journal of the Association of Chartered Physiotherapists in Sports Medicine, 39, 45–51. https://doi.org/10.1016/j.ptsp.2019.06.008

Ferraioli, G., Wong, V. W., Castera, L., Berzigotti, A., Sporea, I., Dietrich, C. F., Choi, B. I., Wilson, S. R., Kudo, M., & Barr, R. G. (2018). Liver Ultrasound Elastography: An Update to the World Federation for Ultrasound in Medicine and Biology Guidelines and Recommendations. Ultrasound in medicine & biology, 44(12), 2419–2440. https://doi-org.ezproxy.jyu.fi/10.1016/j.ultrasmedbio.2018.07.008

Fiorentino, N. M., Rehorn, M. R., Chumanov, E. S., Thelen, D. G. & Blemker, S. S. 2014. Computational Models Predict Larger Muscle Tissue Strains at Faster Sprinting. Medicine & Science in Sports & Exercise 46 (4), 776-786. https://doi.org/10.1249/MSS.0000000000000172

Freitas, S. R., Mendes, B., Firmino, T., Correia, J. P., Witvrouw, E. E. M. C., Oliveira, R., & Vaz, J. R. 2022. Semitendinosus and biceps femoris long head active stiffness response until failure in professional footballers with vs. without previous hamstring injury. European journal of sport science, 22(7), 1132–1140. https://doi.org/10.1080/17461391.2021.1910347

Hatta, T., Giambini, H., Uehara, K., Okamoto, S., Chen, S., Sperling, J. W., Itoi, E., & An, K. N. 2015. Quantitative assessment of rotator cuff muscle elasticity: Reliability and feasibility of shear wave elastography. Journal of biomechanics, 48(14), 3853–3858. https://doi.org/10.1016/j.jbiomech.2015.09.038

Hegyi, A., Goncalves, B. A. M., Finni, T. & Cronin, N. J. 2019. Individual Region- and Muscle-specific Hamstring Activity at Different Running Speeds. Medicine & Science in Sports & Exercise 51 (11), 2274-2285. https://doi.org/10.1249/MSS.0000000000002060

Hegyi, A., Peter, A., Finni, T. & Cronin N. J. 2018. Region-dependent hamstrings activity in Nordic hamstring exercise and stiff-leg deadlift defined with high-density electromyography. Scandinavian Journal of Medicine & Science in Sports 28 (3), 992-1000. https://doi.org/10.1111/sms.13016

Heale, R. & Twycross, A. 2015. Validity and reliability in quantitative studies. Evidence-Based Nursing 18 (3), 66-7. https://doi.org/10.1136/eb-2015-102129

Hinkle, D. E., Wiersma, W., & Jurs, S. G. 2003. Applied statistics for the behavioral sciences (Vol. 663). Boston: Houghton Mifflin.

Hopkins, W.G. 2000. Measures of Reliability in Sports Medicine and Science. Sports Medicine 30, 1–15. https://doi.org/10.2165/00007256-200030010-00001

Joo, I., Kim, S. Y., Park, H. S., Lee, E. S., Kang, H. J. & Lee, J. M. 2019. Validation of a New Point Shear-Wave Elastography Method for Noninvasive Assessment of Liver Fibrosis: A Prospective Multicenter Study, Korean Journal of Radiology 20 (11), 1527–1535. https://doi.org/10.3348/kjr.2019.0109

Kawama, R., Yanase, K., Hojo, T., & Wakahara, T. 2022. Acute changes in passive stiffness of the individual hamstring muscles induced by resistance exercise: effects of contraction mode and range of motion. European journal of applied physiology, 122(9), 2071–2083. https://doi.org/10.1007/s00421-022-04976-6

Kellis, E., Galanis, N., Natsis, K. & Kapetanos, G. 2010. Muscle architecture variations along the human semitendinosus and biceps femoris (long head) length. Journal of Electromyography and Kinesiology 20 (6), 1237-43. https://doi.org/10.1016/j.jelekin.2010.07.012

Kelly, J. P., Koppenhaver, S. L., Michener, L. A., Proulx, L., Bisagni, F., & Cleland, J. A. 2018. Characterization of tissue stiffness of the infraspinatus, erector spinae, and gastrocnemius muscle using ultrasound shear wave elastography and superficial mechanical deformation. Journal of electromyography and kinesiology: official journal of the International Society of Electrophysiological Kinesiology, 38, 73–80. https://doi.org/10.1016/j.jelekin.2017.11.001

Klauser AS, de-Koekkoek F, Schwabl C, Fink C, Friede M, Csapo R. 2022. Intraobserver Assessment of Shear Wave Elastography in Tensor Fasciae Latae and Gluteus Maximus Muscle: The Importance of the Hip Abductor Muscles in Runners Knee Compared to Healthy Controls. Journal of Clinical Medicine.; 11(13):3605. https://doi.org/10.3390/jcm11133605

Koo, T. K., Guo, J. Y., Cohen, J. H., & Parker, K. J. 2014. Quantifying the passive stretching response of human tibialis anterior muscle using shear wave elastography. Clinical biomechanics (Bristol, Avon), 29(1), 33–39. https://doi.org/10.1016/j.clinbiomech.2013.11.009

Koo, T. K. & Li, M.Y. 2016. A guideline of Selecting and Reporting Intraclass Correlation Coefficient for Reliability Research. Journal of Chiropractic Medicine 15, 155-163. https://doi.org/10.1016/j.jcm.2016.02.012

Koppenhaver, S., Kniss, J., Lilley, D., Oates, M., Fernández-de-Las-Peñas, C., Maher, R., Croy, T., & Shinohara, M. 2018. Reliability of ultrasound shear-wave elastography in assessing low back musculature elasticity in asymptomatic individuals. Journal of electromyography and kinesiology : official journal of the International Society of Electrophysiological Kinesiology, 39, 49–57. https://doi.org/10.1016/j.jelekin.2018.01.010

Koulouris, G. & Connell, D. 2005. Hamstring muscle complex: an imaging review. Radiographics 25 (3), 571-86. https://doi.org/10.1148/rg.253045711

Koulouris, G., Connell, D. A. & Brukner, P. 2007. Magnetic Resonance Imaging Parameters for Assessing Risk of Recurrent Hamstring Injuries in Elite Athletes. The American Journal of Sports Medicine 35 (9), 1500-6. https://doi.org/10.1177/0363546507301258

Kozinc, Ž., & Šarabon, N. 2020. Shear-wave elastography for assessment of trapezius muscle stiffness: Reliability and association with low-level muscle activity. PloS one, 15(6), e0234359. https://doi.org/10.1371/journal.pone.0234359

Lee, S. S., Gaebler-Spira, D., Zhang, L. Q., Rymer, W. Z., & Steele, K. M. 2016. Use of shear wave ultrasound elastography to quantify muscle properties in cerebral palsy. Clinical biomechanics (Bristol, Avon), 31, 20–28. https://doi.org/10.1016/j.clinbiomech.2015.10.006

Lee, Y., Kim, M., & Lee, H. 2021. The Measurement of Stiffness for Major Muscles with Shear Wave Elastography and Myoton: A Quantitative Analysis Study. Diagnostics (Basel, Switzerland), 11(3), 524. https://doi.org/10.3390/diagnostics11030524

Le Sant, G., Ates, F., Brasseur, J. L., & Nordez, A. 2015. Elastography Study of Hamstring Behaviors during Passive Stretching. PloS one, 10(9), e0139272. https://doi.org/10.1371/journal.pone.0139272

Le Sant, G., Nordez, A., Andrade, R., Hug, F., Freitas, S. & Gross, R. 2017. Stiffness mapping of lower leg muscles during passive dorsiflexion. Journal of Anatomy 230 (5), 639-650. https://doi.org/10.1111/joa.12589

Lexell, J. E., & Downham, D. Y. 2005. How to assess the reliability of measurements in rehabilitation. American journal of physical medicine & rehabilitation, 84(9), 719–723. https://doi.org/10.1097/01.phm.0000176452.17771.20

Lima, K., Martins, N., Pereira, W., & Oliveira, L. 2017. Triceps surae elasticity modulus measured by shear wave elastography is not correlated to the plantar flexion torque. Muscles, ligaments and tendons journal, 7(2), 347–352. https://doi.org/10.11138/mltj/2017.7.2.347

Liporaci, R. F., Saad, M., Grossi, D. B., & Riberto, M. 2019. Clinical Features and isokinetic Parameters in Assessing Injury Risk in elite Football Players. International journal of sports medicine, 40(14), 903–908. https://doi.org/10.1055/a-1014-2911

Liu, J., Wang, K., Wu, J., Miao, H., Qian, Z., Ren, L., Ren, L. 2020. In Vivo Assessment of Lower Limb Muscle Stress State Based on Shear Wave Elastography, in IEEE Access, vol. 8, pp. 122185-122196, doi: 10.1109/ACCESS.2020.3007145.

Liu, X., Yu, H. K., Sheng, S. Y., Liang, S. M., Lu, H., Gu, L. X., Fu, P., & Pan, M. 2021. Measurement consistency of dynamic stretching muscle stiffness evaluated using shear wave elastography: comparison among different stretched levels and ROI sizes. Medical ultrasonography, 23(1), 55–61. https://doi.org/10.11152/mu-2731

Ma, C. Z., Ren, L. J., Cheng, C. L., & Zheng, Y. P. 2020. Mapping of Back Muscle Stiffness along Spine during Standing and Lying in Young Adults: A Pilot Study on Spinal Stiffness Quantification with Ultrasound Imaging. Sensors (Basel, Switzerland), 20(24), 7317. https://doi.org/10.3390/s20247317

MacDonald, D., Wan, A., McPhee, M., Tucker, K., & Hug, F. 2016. Reliability of Abdominal Muscle Stiffness Measured Using Elastography during Trunk Rehabilitation Exercises.

Ultrasound in medicine & biology, 42(4), 1018–1025. https://doi.org/10.1016/j.ultrasmedbio.2015.12.002

Maganaris, CN., Baltzopoulos, V. & Sargeant AJ. 2002. Repeated contractions alter the geometry of human skeletal muscle. Journal of Applied Physiology 93 (6), 2089–94. https://doi.org/10.1152/japplphysiol.00604.2002

Matsuda, R., Kumamoto, T., Seko, T., Miura, S., & Hamamoto, T. 2019. Reproducibility of elastic modulus measurement of the multifidus using the shear wave elastography function of an ultrasound diagnostic device. Journal of physical therapy science, 31(8), 617–620. https://doi.org/10.1589/jpts.31.617

McPherson, A. L., Nagai, T., Schilaty, N. D., Hale, R., Hewett, T. E., & Bates, N. A. 2020. High school male basketball athletes exhibit greater hamstring muscle stiffness than females as assessed with shear wave elastography. Skeletal radiology, 49(8), 1231–1237. https://doi.org/10.1007/s00256-020-03397-w

Mendes, B., Firmino, T., Oliveira, R., Neto, T., Infante, J., Vaz, J. R., & Freitas, S. R. 2018. Hamstring stiffness pattern during contraction in healthy individuals: analysis by ultrasound-based shear wave elastography. European journal of applied physiology, 118(11), 2403–2415. https://doi.org/10.1007/s00421-018-3967-z

Miyamoto, N., & Hirata, K. 2021. Site-specific features of active muscle stiffness and proximal aponeurosis strain in biceps femoris long head. Scandinavian journal of medicine & science in sports, 31(8), 1666–1673. https://doi.org/10.1111/sms.13973

Miyamoto, N., Hirata, K., & Kanehisa, H. 2017. Effects of hamstring stretching on passive muscle stiffness vary between hip flexion and knee extension maneuvers. Scandinavian journal of medicine & science in sports, 27(1), 99–106. https://doi.org/10.1111/sms.12620

Miyamoto, N., Hirata, K., Kanehisa, H. & Yoshitake, Y. 2015. Validity of measurement of shear modulus by ultrasound shear wave elastography in human pennate muscle. PLoS One 10 (4), e0124311. https://doi.org/10.1371/journal.pone.0124311

Miyamoto, N., Kimura, N., & Hirata, K. 2020. Non-uniform distribution of passive muscle stiffness within hamstring. Scandinavian journal of medicine & science in sports, 30(9), 1729–1738. https://doi.org/10.1111/sms.13732

Mohr, M., Krustrup P. & Bangsbo, J. 2003. Match performance of high-standard soccer players with special reference to development of fatigue. Journal of Sports Sciences 21 (7), 519-528. https://doi.org/10.1080/0264041031000071182

Morel, B., Hug, F., Nordez, A., Pournot, H., Besson, T., Mathevon, L. & Lapole, T. 2019. Reduced Active Muscle Stiffness after Intermittent Submaximal Isometric Contractions. Medicine and Science in Sports and Exercise 51 (12), 2603–2609. https://doi.org/10.1249/MSS.0000000000002080

Morin., J-B., Gimenez, P., Edouard, P., Arnal, P., Jiménez-Reyes, P., Samozino, P., Brughelli, M. ja Mendiguchia, J. 2015. Sprint Acceleration Mechanics: The Major Role of Hamstrings in Horizontal Force Production. Frontiers in Physiology 6, 404. https://doi.org/10.3389/fphys.2015.00404

Nakamura, M., Ikezoe, T., Umegaki, H., Kobayashi, T., Nishisita, S. & Ichihashi, N. 2016. Shear elastic modulus is a reproducible index reflecting the passive mechanical properties of medial gastrocnemius muscle belly. Acta Radiologica Open 5 (4), 1-6. https://doi.org/10.1177/2058460115604009

Oliveira, V. B., Carneiro, S. P., & Oliveira, L. F. 2016. Reliability of biceps femoris and semitendinosus muscle architecture measurements obtained with ultrasonography. Research on Biomedical Engineering, 32(4), 365–371. https://doi.org/10.1590/2446-4740.04115

Opar, D. A., Piatkowski, T., Williams, M. D., & Shield, A. J. 2013. A novel device using the Nordic hamstring exercise to assess eccentric knee flexor strength: a reliability and retrospective injury study. The Journal of orthopaedic and sports physical therapy, 43(9), 636–640. https://doi.org/10.2519/jospt.2013.4837

Opar, D. A., Williams, M. D. & Shield, A. J. 2012. Hamstring Strain Injuries: Factors that Lead to Injury and Re-Injury. Sports Medicine 42 (3), 209-26. https://doi.org/10.2165/11594800-000000000-00000

Pałac M. & Linek P. 2022. Intra-Rater Reliability of Shear Wave Elastography for the Quantification of Respiratory Muscles in Adolescent Athletes. Sensors. 22(17):6622. https://doi.org/10.3390/s22176622

Phan, A., Lee, J., & Gao, J. 2019. Ultrasound shear wave elastography in assessment of skeletal muscle stiffness in senior volunteers. Clinical imaging, 58, 22–26. https://doi.org/10.1016/j.clinimag.2019.06.006

Pimenta, R., Coelho, F., Correia, J. P., & Vaz, J. R. (2024). Influence of transducer pressure and examiner experience on muscle active shear modulus measured by shear wave elastography. Radiography (London, England : 1995), 30(1), 185–192. https://doi.org/10.1016/j.radi.2023.11.005

Putz, R., Pabst, R. & Sobotta, J. 2010. e-Sobotta, Atlas of Human Anatomy, Tables. 15 painos. München, Elsevier Urban & Fischer.

Putz, R., Pabst, R. & Sobotta, J. 2009. Sobotta, Atlas of Human Anatomy. 14 painos. München, Elsevier Urban & Fischer.

Rodgers, C. D. & Raja, A. 2019. Anatomy, Bony Pelvis and Lower Limb, Hamstring Muscle. StatPearls Publishing. https://www.ncbi.nlm.nih.gov/books/NBK546688/

Rosskopf, A. B., Ehrmann, C., Buck, F. M., Gerber, C., Flück, M. & Pfirrmann, C. W. A. 2016. Quantitative Shear-Wave US Elastography of the Supraspinatus Muscle: Reliability of the Method and Relation to Tendon Integrity and Muscle Quality. Radiology 278 (2), 465-74. https://doi.org/10.1148/radiol.2015150908

Ruby, L., Mutschler, T., Martini, K., Klingmüller, V., Frauenfelder, T., Rominger, M. B., & Sanabria, S. J. 2019. Which Confounders Have the Largest Impact in Shear Wave Elastography of Muscle and How Can They be Minimized? An Elasticity Phantom, Ex Vivo Porcine Muscle and Volunteer Study Using a Commercially Available System. Ultrasound in medicine & biology, 45(10), 2591–2611. https://doi.org/10.1016/j.ultrasmedbio.2019.06.417

Ryu, JA. & Jeong, WK. 2017. Current status of musculoskeletal application of shear wave elastography. Ultrasonography 36 (3), 185-197. https://doi.org/10.14366/usg.16053

Saeki, J., Ikezoe, T., Nakamura, M., Nishishita, S., & Ichihashi, N. 2017. The reliability of shear elastic modulus measurement of the ankle plantar flexion muscles is higher at dorsiflexed position of the ankle. Journal of foot and ankle research, 10, 18. https://doi.org/10.1186/s13047-017-0199-0

Sarto, F., Spörri, J., Fitze, D. P., Quinlan, J. I., Narici, M. V., & Franchi, M. V. 2021. Implementing Ultrasound Imaging for the Assessment of Muscle and Tendon Properties in Elite Sports: Practical Aspects, Methodological Considerations and Future Directions. Sports medicine (Auckland, N.Z.), 51(6), 1151–1170. https://doi.org/10.1007/s40279-021-01436-7

Šarabon, N., Kozinc, Ž., & Podrekar, N. 2019. Using shear-wave elastography in skeletal muscle: A repeatability and reproducibility study on biceps femoris muscle. PloS one, 14(8), e0222008. https://doi.org/10.1371/journal.pone.0222008

Sarvazyan A. P., Rudenko O. V., Swanson S., Fowlkes J. B., Stanislavy A. & Emelianov S. Y. 1998. Shear Wave Elasticity Imaging: A New Ultrasonictechnology Of Medical Diagnostics Ultrasound in Medicine & Biology 24 (9), 1419 –1435. ttps://doi.org/10.1016/s0301-5629(98)00110-0

Savolainen, E. H. J., Vänttinen, T., Ihalainen, J. K., & Walker, S. 2023. Physical qualities and body composition predictors of running performance in national level women's official soccer matches. Biology of sport, 40(4), 1187–1195. https://doi.org/10.5114/biolsport.2023.118026

Shiina, T., Nightingale, K., Palmeri, M., Hall, T., Bamber, J., Barr, R., Castera, L., Choi, B., Chou, Y., Cosgrove, D., Dietrich C., Ding, H., Amy, D., Farrokh, A., Ferraioli, G., Filice, C., Friedrich-Rust, M., Nakashima, K., Schafer, F., Sporea, I., Suzuki, S., Wilson, S. & Kudo, M. 2015. WFUMB guidelines and recommendations for clinical use of ultrasound elastography: Part 1: basic principles and terminology. Ultrasound in Medicine & Biology, 41 (5), 1126-47.

Sigrist, R. M. S, Liau, J., El Kaffas, A., Chammas, M. C. & Willmann, J. K. 2017. Ultrasound Elastography: Review of Techniques and Clinical Applications. Theranostics 7 (5), 1303-1329. https://doi.org/10.7150/thno.18650

Siracusa, J., Charlot, K., Malgoyre, A., Conort, S., Tardo-Dino, P., Bourrilhon, C. & Garcia-Vicencio, S. 2019. Resting Muscle Shear Modulus Measured with Ultrasound Shear-Wave Elastography as an Alternative Tool to Assess Muscle Fatigue in Humans. Frontiers in Physiology 10, 626, 10.3389. https://doi.org/10.3389/fphys.2019.00626

Stepien, K., Smigielski, R., Mouton, C., Ciszek, B., Engelhardt, M. & Seil, R. 2018. Anatomy of proximal attachment, course, and innervation of hamstring muscles: a pictorial essay. Knee Surgery, Sports Traumatology, Arthroscopy 27 (3), 673-684. https://doi.org/10.1007/s00167-018-5265-z

Storey, R., Stringer, M., & Woodley, S. J. 2012. Site of acute hamstring strains and activities associated with injury: A systematic review. Official Journal of Sports Medicine New Zealand Inc. 39 (2), 36-40.

Sukanen, M., Khair, R. M., Ihalainen, J. K., Laatikainen-Raussi, I., Eon, P., Nordez, A., & Finni, T. 2023. Achilles tendon and triceps surae muscle properties in athletes. European journal of applied physiology, 10.1007/s00421-023-05348-4. Advance online publication. https://doi.org/10.1007/s00421-023-05348-4

Taljanovic, M. S., Gimber, L. H., Becker, G. W., Latt, L. D., Klauser, A. S., Melville, D. M., Gao, L. & Witte, R. S. 2017. Shear-Wave Elastography: Basic Physics and Musculoskeletal Applications. RadioGraphics 37, 855–870. https://doi.org/10.1148/rg.2017160116

Taş, S., Onur, M. R., Yılmaz, S., Soylu, A. R., & Korkusuz, F. 2017. Shear Wave Elastography Is a Reliable and Repeatable Method for Measuring the Elastic Modulus of the Rectus Femoris Muscle and Patellar Tendon. Journal of ultrasound in medicine : official journal of the American Institute of Ultrasound in Medicine, 36(3), 565–570. https://doi.org/10.7863/ultra.16.03032

Temfemo, A., Hugues, J., Chardon, K., Mandengue, S. H., & Ahmaidi, S. 2009. Relationship between vertical jumping performance and anthropometric characteristics during growth in boys and girls. European journal of pediatrics, 168(4), 457–464. https://doi.org/10.1007/s00431-008-0771-5

Thelen, D., Chumanov, E., Hoerth, D., Best, T., Swanson, S., Li, L., Young, M. & Heiderscheit, B. 2005. Hamstring muscle kinematics during treadmill sprinting. Medicine and Science in Sports and Exercise 37 (1), 108-14. https://doi.org/10.1249/01.mss.0000150078.79120.c8

Tier, L., Salomoni, S. E., Hug, F., Besomi, M., & Hodges, P. W. 2021. Shear modulus of multifidus and longissimus muscles measured using shear wave elastography correlates with muscle activity, but depends on image quality. Journal of electromyography and kinesiology: official journal of the International Society of Electrophysiological Kinesiology, 56, 102505. https://doi.org/10.1016/j.jelekin.2020.102505

Timmins, R., Bourne, M., Shield, A., Williams, Lorenzen & Opar. 2016. Short biceps femoris fascicles and eccentric knee flexor weakness increase the risk of hamstring injury in elite football (soccer): a prospective cohort study, British Journal of Sports Medicine 50 (24), 1524-1535. https://doi.org/10.1136/bjsports-2015-095362

Timmins, R. G., Shield, A. J., Williams, M. D., Lorenzen, C., & Opar, D. A. 2015. Biceps femoris long head architecture: a reliability and retrospective injury study. Medicine and science in sports and exercise, 47(5), 905–913. https://doi.org/10.1249/MSS.0000000000000507

Timmins, R., Woodley, S., Shield, A., ja Opar, D. 2020. Anatomy of the Hamstrings. In Thorborg, K., Opar, D. & Shield, A. Prevention and Rehabilitation of Hamstring Injuries. Frontiers in Physiology 6, 404, 1-30.

Tosovic, D., Muirhead, J. C., Brown, J. M., & Woodley, S. J. 2016. Anatomy of the long head of biceps femoris: An ultrasound study. Clinical anatomy (New York, N.Y.), 29(6), 738–745. https://doi.org/10.1002/ca.22718

Van Hooren, B., Aagaard, P., Monte, A., & Blazevich, A. J. 2024. The role of pennation angle and architectural gearing to rate of force development in dynamic and isometric muscle contractions. Scandinavian journal of medicine & science in sports, 34(5), e14639. https://doi.org/10.1111/sms.14639

Verrall, G. M., Slavotinek, J. P., Barnes, P. G. & Fon G. T. 2003. Diagnostic and prognostic value of clinical findings in 83 athletes with posterior thigh injury. Comparison of clinical findings with magnetic resonance imaging documentation of hamstring muscle strain. American Journal of Sports Medicine 31(6), 969–73. https://doi.org/10.1177/03635465030310063701

Vuorenmaa, A. S., Siitama, E. M. K., & Mäkelä, K. S. 2022. Inter-operator and inter-device reproducibility of shear wave elastography in healthy muscle tissues. Journal of applied clinical medical physics, 23(9), e13717. https://doi.org/10.1002/acm2.13717

Waldén, M., Hägglund, M., Werner, J., & Ekstrand, J. 2011. The epidemiology of anterior cruciate ligament injury in football (soccer): a review of the literature from a gender-related perspective. Knee surgery, sports traumatology, arthroscopy : official journal of the ESSKA, 19(1), 3–10. https://doi.org/10.1007/s00167-010-1172-7

Wang, X., Hu, Y., Zhu, J., Gao, J., Chen, S., Liu, F., Li, W., Liu, Y., & Ariun, B. 2020. Effect of acquisition depth and precompression from probe and couplant on shear wave elastography in soft tissue: an in vitro and in vivo study. Quantitative imaging in medicine and surgery, 10(3), 754–765. https://doi.org/10.21037/qims.2020.01.15

Woodley, S., J. & Mercer, S. R. 2005. Hamstring Muscles: Architecture and Innervation. Cells Tissues Organs 179, 125–141. https://doi.org/10.1159/000085004

Wu, J., Qian, Z., Liang, W., Liu, J., Ren, L., & Ren, L. 2020. In vivo assessment of material properties of muscles and connective tissues around the knee joint based on shear wave elastography. Journal of the mechanical behavior of biomedical materials, 109, 103829. https://doi.org/10.1016/j.jmbbm.2020.103829

Xie, Y., Thomas, L., Hug, F., Johnston, V., & Coombes, B. K. 2019. Quantifying cervical and axioscapular muscle stiffness using shear wave elastography. Journal of electromyography and kinesiology: official journal of the International Society of Electrophysiological Kinesiology, 48, 94–102. https://doi.org/10.1016/j.jelekin.2019.06.009

Yamazaki, K., Inoue, K., & Miyamoto, N. (2022). Passive and active muscle elasticity of medial gastrocnemius is related to performance in sprinters. European journal of applied physiology, 122(2), 447–457. https://doi.org/10.1007/s00421-021-04848-5

Young, B. A., Koppenhaver, S. L., Timo-Dondoyano, R. M., Baumann, K., Scheirer, V. F., Wolff, A., Sutlive, T. G., & Elliott, J. M. 2021. Ultrasound shear wave elastography measurement of the deep posterior cervical muscles: Reliability and ability to differentiate between muscle contraction states. Journal of electromyography and kinesiology: official journal of the International Society of Electrophysiological Kinesiology, 56, 102488. https://doi.org/10.1016/j.jelekin.2020.102488

Yu, B., Queen, R. M., Abbey, A. N., Liu, Y., Moorman, C. T. & Garrett, W. E. 2008. Hamstring muscle kinematics and activation during overground sprinting. Journal of Biomechanics 41 (15), 3121-3126. https://doi.org/10.1016/j.jbiomech.2008.09.005